SpezialForschungsBereich F 32

Karl–Franzens Universität Graz
Technische Universität Graz
Medizinische Universität Graz

SPACE MAPPING TECHNIQUES FOR A STRUCTURAL OPTIMIZATION PROBLEM GOVERNED BY THE p-LAPLACE EQUATION

O. Lass C. Posch G. Scharrer

S. Volkwein

SFB-Report No. 2009–023 May 2009

A–8010 GRAZ, HEINRICHSTRASSE 36, AUSTRIA

Supported by the
Austrian Science Fund (FWF)

Der Wissenschaftsfonds.

SFB sponsors:

- **Austrian Science Fund** (FWF)
- **University of Graz**
- **Graz University of Technology**
- **Medical University of Graz**
- **Government of Styria**
- **City of Graz**

SPACE MAPPING TECHNIQUES FOR A STRUCTURAL OPTIMIZATION PROBLEM GOVERNED BY THE p-LAPLACE EQUATION

O. LASS, C. POSCH, G. SCHARRER, AND S. VOLKWEIN

Abstract. Solving optimal control problems for real world applications are hard to tackle numerically due to the large size and the complex underlying (partial differential equations based) models. In this paper a structural optimization problem governed by the p-Laplace equation (fine model) is considered. A surrogate optimization is utilized to develop an efficient numerical optimization method. Here the p-Laplace equation is replaced by a simplified (coarse) model, a space mapping attempts to match, in the coarse model, the values of the p-Laplace equation. Numerical examples illustrate the presented approach.

1. Introduction

A main aspect in the design of passenger cars with respect to pedestrian safety is the energy absorption capability of the engine hood. Besides that, the hood has to fulfill several other requirements. That makes it necessary to develop easy and fast to solve prediction models with little loss in accuracy for optimization purpose. Current simulation tools combined with standard optimization software are not well suited to deal with the above mentioned needs.

The present paper shows the application of mathematical methods on a simplified model to reduce the optimization effort. We continue the work in [20] and consider a structural optimization problem. The optimization variables are a thickness parameter λ of a plate $\Omega \subset \mathbb{R}^2$ (representing a part of the vehicle) and an associated displacement u satisfying the *p-Laplace equation*

$$-\mathrm{div}\left(2(1+n)\lambda(\mathbf{x})\,|\nabla u(\mathbf{x})|_2^{2n}\,\nabla u(\mathbf{x})\right) = g(\mathbf{x}) \quad \text{for all } \mathbf{x} \in \Omega \tag{1.1}$$

together with homogeneous Dirichlet boundary conditions, where g represents a force acting on Ω, $n \in (0, 1)$ is the Hollomon coefficient, and $|\cdot|_2$ stands for the Euclidean norm. Equation (1.1) is a quasilinear, elliptic partial differential equation (PDE). We suppose that $0 < \lambda_a \le \lambda(\mathbf{x}) \le \lambda_b$ with positive scalars λ_a, λ_b. Our goal is to minimize the mass of the plate, i.e., to minimize the integral

$$J_1(\lambda) = \int_\Omega \lambda(\mathbf{x})\,\mathrm{d}\mathbf{x}$$

Date: May 30, 2009.

Key words and phrases. p-Laplace equation, optimal control, space mapping, surrogate optimization, globalized Newton-CG method.

The authors gratefully acknowledge support by the Zukunftsfonds des Landes Steiermark under grant no. 4120.

but also to avoid that the displacement u is larger than a given threshold $u_b > 0$. This issue is motivated by our pedestrian safety application. Thus, we choose

$$J_2(u) = \beta \int_\Omega \min(u(\mathbf{x}) - u_b, 0)^3 \, \mathrm{d}\mathbf{x}$$

as the second part of our cost functional. Here. $\beta > 0$ is a weighting parameter. Clearly, the choice $\lambda = \lambda_a$ minimizes J_1. On the other hand, a small thickness parameter λ causes a large displacement u computed from (1.1). Due to the quasilinear structure, the numerical solution of the optimization problem governed by the PDE constraint (1.1) is expensive, we consider an alternative constraint given by

$$-\mathrm{div}\left(2(1+n)\lambda(\mathbf{x})\,\nabla u(\mathbf{x})\right) = g(\mathbf{x}) \quad \text{for all } \mathbf{x} \in \Omega, \tag{1.2}$$

which is a linear elliptic PDE. We will call (1.1) the *fine model* and (1.2) the *coarse model*. It turns out that the space-mapping technique [15] provides an attractive framework to improve the use of the coarse model as a surrogate for the optimization of the fine model. For that purpose the space mapping is defined, attemps to match, in the coarse model, the fine model displacement values and/or their responses.

The space mapping approach was introduced in [5]. The idea of the space mapping has been developed along different directions and generalized to a number of contexts. One of the problems lies in the information necessary to compute the Jacobian of the space mapping which involves expensive gradient information of (1.1). In [6] Broyden's method is utilized to construct an approximation of the Jacobian. This approach will be used in our paper. Trust-region methods for the surrogate optimization are applied in [4, 22]. In the context of PDEs, we refer to [12], where a modified Broyden formula is presented. Let us mention that optimal control problem for the p-Laplace equation were considered, e.g., in [7, 8].

The paper is organized in the following manner: In Section 2 we introduce the optimal control problem for the p-Laplace equation. The optimal control problem for the coarse model (1.2) is analyzed in Section 3. Moreover, for the numerical solution a globalized Newton-CG method is utilized [18]. Section 4 is devoted to the definition of the space mapping, its numerical realization, and its use in the surrogate optimization. Finally, in the Appendix we present the proofs.

2. Optimization of the complex model

Motivated by the car safety application, we introduce an optimal control problem governed by the p-Laplace equation. Since the p-Laplace equation is a quasilinear, elliptic PDE, the numerical solution of the optimal control problem is expensive. In the context of the surrogate optimization the p-Laplace equation is the fine (accurate, but complex) model.

2.1. The p-Laplacian equation. Let $\Omega \subset \mathbb{R}^d$, $d \in \{2, 3\}$ denote an open and bounded domain with boundary $\Gamma = \partial\Omega$. By $L^q(\Omega)$ we denote the common Lebesgue spaces

$$L^q(\Omega) = \left\{ \varphi : \Omega \to \mathbb{R} \,\middle|\, \varphi \text{ is measurable and } \int_\Omega \left|\varphi(\mathbf{x})\right|^q \mathrm{d}\mathbf{x} < \infty \right\}, \quad 1 \le q < \infty,$$

$$L^\infty(\Omega) = \left\{ \varphi : \Omega \to \mathbb{R} \,\middle|\, \varphi \text{ is measurable and } \operatorname*{ess\,sup}_{\mathbf{x}\in\Omega} \left|\varphi(\mathbf{x})\right| \right\}.$$

In particular, $L^2(\Omega)$ is the space of square-integrable functions in Ω. We endow $L^2(\Omega)$ by the usual inner product and the induced norm. Moreover, we recall the Sobolev space

$$W_0^{1,q}(\Omega) = \Big\{ \varphi \in L^q(\Omega) \,\Big|\, \varphi = 0 \text{ on } \Gamma \text{ and } \int_\Omega |\nabla \varphi(\mathbf{x})|_2^q \,\mathrm{d}\mathbf{x} < \infty \Big\}, \quad 1 \le q < \infty,$$

where $|\cdot|_2$ denotes the Euclidian norm in $\mathbb{R}^d$. For $q = 2$ we set $H_0^1(\Omega) = W_0^{1,2}(\Omega)$ and $V = H_0^1(\Omega)$, which is a Hilbert space supplied with the inner product

$$\langle \varphi, \psi \rangle_V = \int_\Omega \varphi(\mathbf{x})\psi(\mathbf{x}) + \nabla\varphi(\mathbf{x}) \cdot \nabla\psi(\mathbf{x}) \,\mathrm{d}\mathbf{x} \quad \text{for } \varphi, \psi \in V$$

and the induced norm $\|\varphi\|_V = \sqrt{\langle \varphi, \varphi \rangle_V}$ for $\varphi \in V$. We refer the reader, e.g., to [1, 11] for more details on Lebesgue and Sobolev spaces.

Let $n \in (0, 1)$ be the Hollomon coefficient. Suppose that the thickness parameter $\lambda \in L^\infty(\Omega)$ satisfies $\lambda(\mathbf{x}) \ge t_a$ for almost all (f.a.a.) $\mathbf{x} \in \Omega$ and for a positive scalar λ_a. Moreover, let $g : \Omega \to \mathbb{R}$ be a given force term. Then, the displacement satisfies the non-linear, elliptic PDE

$$\begin{aligned} -\mathrm{div}\left(2(1+n)\lambda(\mathbf{x})\,|\nabla u(\mathbf{x})|_2^{2n}\,\nabla u(\mathbf{x})\right) &= g(\mathbf{x}) \quad \text{f.a.a. } \mathbf{x} \in \Omega, \\ u(\mathbf{x}) &= 0 \qquad \text{f.a.a. } \mathbf{x} \in \Gamma. \end{aligned} \tag{2.1}$$

We set $p = 2n + 2$ and $q = (2n + 2)/(2n + 1)$. Then,

$$p \in (2, 4), \quad q \in \left(\frac{4}{3}, 2\right), \quad \frac{1}{p} + \frac{1}{q} = 1,$$

and (2.1) can be written in the standard form of the p-Laplace equation

$$-\mathrm{div}\left(2(1+n)\lambda(\mathbf{x})\,|\nabla u(\mathbf{x})|_2^{p-2}\,\nabla u(\mathbf{x})\right) = g(\mathbf{x}) \qquad \text{f.a.a. } \mathbf{x} \in \Omega, \tag{2.2a}$$

$$u(\mathbf{x}) = 0 \qquad \text{f.a.a. } \mathbf{x} \in \Gamma. \tag{2.2b}$$

Remark 2.1.
1) The p-Laplace equation appears in many physical models (steady laminar flows of non-Newtonian fluids, some reaction-diffusion problems, magnetostatics, glaciology); see, e.g., [2, 3, 9].
2) If $|\nabla u(\mathbf{x})|_2 = 0$ almost everywhere (a.e.) on a subset of Ω, (2.2a) becomes a singular equation. Therefore, instead of (2.2) we solve

$$\begin{aligned} -\mathrm{div}\left(2(1+n)\lambda(\mathbf{x})\,(\varepsilon + |\nabla u(\mathbf{x})|_2)^{p-2}\,\nabla u(\mathbf{x})\right) &= g(\mathbf{x}) \quad \text{f.a.a. } \mathbf{x} \in \Omega, \\ u(\mathbf{x}) &= 0 \qquad \text{f.a.a. } \mathbf{x} \in \Gamma \end{aligned} \tag{2.3}$$

in our numerical experiments, where $0 < \varepsilon \ll 1$ is a small scalar. For $\lambda \ge \lambda_a$ in Ω a.e. we infer from $\varepsilon > 0$ that

$$2(1+n)\lambda(\mathbf{x})(\varepsilon + |\nabla u(\mathbf{x})|_2)^{p-2} \ge 2(1+n)\lambda_a \varepsilon^{p-2} > 0 \quad \text{f.a.a. } \mathbf{x} \in \Omega,$$

so that (2.3) has a positive diffusion parameter. ◊

We call u a *weak solution to* (2.2) if $u \in W_0^{1,p}(\Omega)$ holds and u satisfies

$$\int_\Omega 2(1+n)\lambda(\mathbf{x})\,|\nabla u(\mathbf{x})|_2^{p-2}\,\nabla u(\mathbf{x}) \cdot \nabla\varphi(\mathbf{x}) \,\mathrm{d}\mathbf{x} = \int_\Omega g(\mathbf{x})\varphi(\mathbf{x}) \,\mathrm{d}\mathbf{x} \tag{2.4}$$

for all $\varphi \in W_0^{1,p}(\Omega)$.

Theorem 2.2. *Suppose that the thickness parameter $\lambda \in L^\infty(\Omega)$ satisfies $\lambda(\mathbf{x}) \ge \lambda_a$ f.a.a. $\mathbf{x} \in \Omega$ and for a positive scalar λ_a. Let $g \in L^2(\Omega)$. Then,* (2.2) *possesses a unique weak solution u.*

Proof. The boundedness of Ω and $g \in L^2(\Omega)$ imply that $g \in L^q(\Omega)$ for $q = (2n+2)/(2n+1) \in (4/3, 2)$. Note that (2.4) is the Euler equation for the minimization problem

$$\min_{u \in W_0^{1,p}(\Omega)} \frac{1}{p} \int_\Omega 2(n+1)\lambda(\mathbf{x}) \big|\nabla u(\mathbf{x})\big|_2^p - g(\mathbf{x})u(\mathbf{x})\,\mathrm{d}\mathbf{x}.$$

Now the existence of a weak solution follows from Proposition II.1.2 in [10]. The uniqueness follows from the fact that the functional

$$u \mapsto \int_\Omega 2(n+1)\lambda(\mathbf{x}) \big|\nabla u(\mathbf{x})\big|_2^p \,\mathrm{d}\mathbf{x}$$

is strictly convex for $p = 2n + 2 > 1$. □

Corollary 2.3. *Let all assumption of Theorem* 2.2 *hold and* $p = 2n+2$. *Then, the weak solution* u *lies in* $L^\infty(\Omega)$ *and satisfies*

$$\|u\|_{W^{1,p}(\Omega)} + \|u\|_{L^\infty(\Omega)} \le C$$

for a constant $C > 0$ *depending on* n, λ_a, $\|\lambda\|_{L^\infty(\Omega)}$, *and* $\|g\|_{L^2(\Omega)}$.

Proof. Since $\lambda(\mathbf{x}) \ge \lambda_a$ f.a.a. $\mathbf{x} \in \Omega$, the claim follows from [8, Theorem 2.3]. □

Let us define the Banach space $X = L^\infty(\Omega) \times \big(W_0^{1,p}(\Omega) \cap L^\infty(\Omega)\big)$ and the non-linear operator $f : X \to W_0^{1,p}(\Omega)'$ as

$$\langle f(x), \varphi\rangle_{(W_0^{1,p})', W_0^{1,p}} = \int_\Omega 2(1+n)\lambda(\mathbf{x})|\nabla u(\mathbf{x})|_2^{p-2}\nabla u(\mathbf{x}) \cdot \nabla\varphi(\mathbf{x}) - g(\mathbf{x})\varphi(\mathbf{x})\,\mathrm{d}\mathbf{x}$$

for $x = (\lambda, u) \in X$ and $\varphi \in W_0^{1,p}(\Omega)$, where $\langle\cdot\,,\cdot\rangle_{(W_0^{1,p})', W_0^{1,p}}$ denotes the dual pairing between $W_0^{1,p}(\Omega)'$ and $W_0^{1,p}(\Omega)$. Now, $f(x) = 0$ in $W_0^{1,p}(\Omega)'$ for $x = (\lambda, u) \in X$ is equivalent with the fact that u is a weak solution to (2.2) for thickness parameter λ.

2.2. Numerical solution of the *p*-Laplace equation. In this section we present numerical solutions of the p-Laplace equation for two different types of thickness parameter λ on a two-dimensional domain. We utilize piecewise linear finite element (FE) ansatz functions for the spatial variable. Let $\{\varphi_i\}_{i=1}^{N_{fe}}$ denote the N_{fe} FE ansatz functions and $\{\mathbf{x}_i\}_{i=1}^{N_{fe}}$ the grid points in $\overline{\Omega}$ such that $\varphi_i(\mathbf{x}_i) = 1$ for $1 \le i \le N_{fe}$ and $\varphi_i(\mathbf{x}_j) = 0$ for $i \ne j$. For this we apply the MATLAB PARTIAL DIFFERENTIAL EQUATION TOOLBOX inbuilt function `pdenonlin` on the regularized problem (2.3) with $N_{fe} = 2023$ degrees of freedom. The `pdenonlin` routine uses Gauss-Newton iterations to solve the non-linear equations

$$r(u_h(\mathbf{x}_i)) = -\mathrm{div}\left(2(1+n)\lambda(\mathbf{x}_i)\left(\varepsilon + |\nabla u_h(\mathbf{x}_i)|_2\right)^{p-2}\nabla u_h(\mathbf{x}_i)\right) - g(\mathbf{x}_i) = 0$$

for $1 \le i \le N_{fe}$, where u_h denotes the FE solution. The Gauss-Newton method only converges when the initial guess for $u(\mathbf{x})$ is close enough to the solution. To improve convergence from bad initial guesses the MATLAB routine implements the Armijo-Goldstein line search as damping strategy for choosing the step size. The parameter `norm` is set to 2 (Euclidean norm) and `tol` is set to 10^{-6}. For all other parameters the default values are used.

The Hollomon coefficient is set to $n = 0.22$ and ε is 10^{-10}. Then, $p = 2.44$ in (2.3) The right-hand side g (force term) is given as follows:

$$g(\mathbf{x}) = \begin{cases} 47.71, & \mathbf{x} \in \mathcal{B}_r(\mathbf{x}_{mid}) = \left\{ \mathbf{x} \in \Omega \,\middle|\, |\mathbf{x}_{mid} - \mathbf{x}|_2 < r \right\}, \\ 0, & \text{otherwise}, \end{cases} \tag{2.5}$$

where $\mathbf{x}_{mid} = (0.5, 0.45)^T$ and $r = 0.1$. The value 47.71 (Newton) corresponds approximately the mass of a human head ($4.86\,kg$).

Run 2.1. In the first experiment, $\lambda(\mathbf{x})$ is set to a constant value of 0.75, see Figure 2.1 (left plot). The `pdenonlin` algorithm needs 10 iterations to terminate.

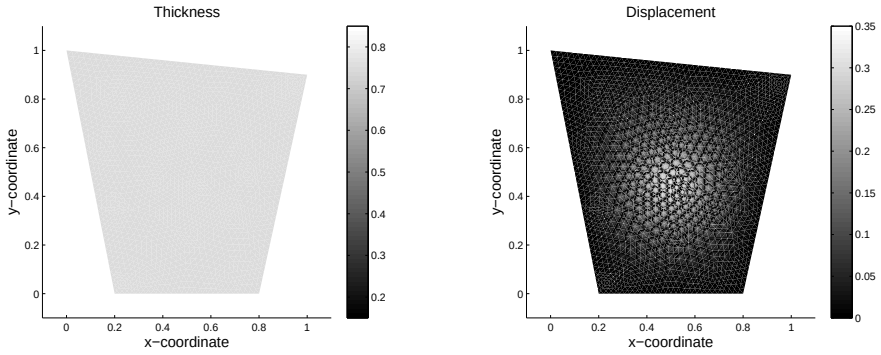

FIGURE 2.1. Run 2.1: Constant thickness parameter λ (left plot) and corresponding weak solution u to the p-Laplace equation (right plot).

The weak solution to (2.3) is presented in the right plot in Figure 2.1. ◊

Run 2.2. For the second experiment, $\lambda(\mathbf{x})$ is generated with a non-constant thickness parameter, see Figure 2.2 (left plot). Again, the `pdenonlin` algorithm stops

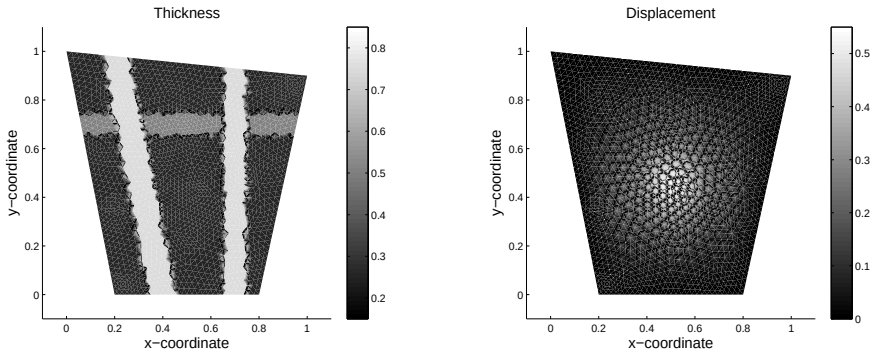

FIGURE 2.2. Run 2.2: Non-constant thickness parameter λ (left plot) and and corresponding weak solution u to the p-Laplace equation (right plot).

after 10 iterations. The obtained weak solution is presented in the right plot in Figure 2.2. ◊

2.3. The optimal control problem. Let $\Phi : \mathbb{R} \to [0, \infty)$ satisfy $\Phi(s) = 0$ for $s \leq 0$ and $\Phi(s) > 0$ for $s > 0$. To ensure differentiability of the cost we require that $\Phi \in C^2(\mathbb{R})$.

The goal is to determine an optimal thickness parameter λ and a corresponding optimal displacement u minimizing the cost functional $J : X \to \mathbb{R}$ given by

$$J(x) = \int_\Omega \lambda(\mathbf{x}) + \frac{\eta}{2} \left|\lambda(\mathbf{x}) - \lambda^\circ(\mathbf{x})\right|^2 + \beta\, \Phi\big(u(\mathbf{x}) - u_b(\mathbf{x})\big)\, \mathrm{d}\mathbf{x}$$

for $x = (\lambda, u) \in X$ subject to the equality constraints $e(x) = 0$ in $W_0^{1,p}(\Omega)'$ and to the inequality constraints

$$\lambda_a \leq \lambda(\mathbf{x}) \leq \lambda_b \quad \text{f.a.a. } \mathbf{x} \in \Omega,$$

where λ_a, λ_b are positive scalars with $\lambda_a \leq \lambda_b$, $\eta \geq 0$ is a regularization parameter and $\lambda^\circ \in L^\infty(\Omega)$ is a nominal thickness parameter satisfying $\lambda_a \leq \lambda^\circ(\mathbf{x}) \leq \lambda_b$ f.a.a. $\mathbf{x} \in \Omega$. Furthermore, $\beta \geq 0$ is a weighting parameter and $u_b \in L^\infty(\Omega)$ satisfies $u_b(\mathbf{x}) > 0$ f.a.a. $\mathbf{x} \in \Omega$. The second term of the cost functional J penalizes the situation if the displacement is larger then the given threshold u_b.

Remark 2.4. In the numerical experiments we choose $\Phi(s) = \max(s, 0)^3/3$ for $s \in \mathbb{R}$. Then, $\Phi \in C^2(\mathbb{R})$. $\lozenge$

We introduce the set of admissible thickness parameters by

$$\Lambda_{ad} = \big\{\lambda \in L^2(\Omega) \,|\, \lambda_a \leq \lambda(\mathbf{x}) \leq \lambda_b \text{ f.a.a. } \mathbf{x} \in \Omega\big\} \tag{2.6}$$

and define $X_{ad} = \Lambda_{ad} \times \big(W_0^{1,p}(\Omega) \cap L^\infty(\Omega)\big)$. Moreover, the set of admissible solutions is

$$\mathcal{F}(\mathbf{P}_f) = \big\{x \in X_{ad} \,\big|\, f(x) = 0 \text{ in } W_0^{1,p}(\Omega)'\big\}.$$

Now the minimization problem can be formulated abstractly as

$$\min J(x) \quad \text{subject to (s.t.)} \quad x \in \mathcal{F}(\mathbf{P}_f). \tag{$\mathbf{P}_f$}$$

Let us refer to [7, 8], where a Dirichlet and Neumann optimal control problem governed by the p-Laplace equation is considered. The authors prove existence of solutions and derive optimality conditions. Moreover, they also include integral state constraints in their model problem.

We proceed by formulating the reduced problem for ($\mathbf{P}_f$). Motivated by Theorem 2.2 and Corollary 2.3 we define the non-linear and bounded solution operator $S : \Lambda_{ad} \to W_0^{1,p}(\Omega) \cap L^\infty(\Omega)$ as follows: $u = S(\lambda)$ is the unique weak solution to (2.2). Then, we introduce the reduced cost functional

$$\hat{J}(\lambda) = J(\lambda, S(\lambda)) \quad \text{for } \lambda \in \Lambda_{ad}$$

and study the reduced problem

$$\min \hat{J}(\lambda) \quad \text{s.t.} \quad \lambda \in \Lambda_{ad}. \tag{$\hat{\mathbf{P}}_f$}$$

We suppose that ($\hat{\mathbf{P}}_f$) admits at least one local solution λ^*. Then, $x^* = (\lambda^*, u^*)$ with $u^* = S(\lambda^*)$ is a local solution to ($\mathbf{P}_f$).

Solving ($\hat{\mathbf{P}}_f$) numerically is a difficult task due to the quasilinear elliptic constraint $f(x) = 0$ (fine model). In the next section we utilize instead of the accurate, but complex model (2.2) a linear elliptic PDE as a simpler model that is much easier to solve. Then, we combine the simple and the complex model by applying a space mapping approach (see Section 4).

3. Optimization of the simpler model

Due to the quasi-linear PDE constraint the numerical solution of $(\hat{\mathbf{P}}_f)$ is expensive. This section is devoted to analyze the optimal control problem, where, in contrast to $(\hat{\mathbf{P}}_f)$, the PDE constraint is a linear elliptic PDE. We prove existence of optimal solutions and derive first- as well as second-order optimality conditions. Moreover, numerical experiments are included. Compared to the previous section, we write μ for the thickness parameter (instead of λ in Section 2) and v for the displacement (instead of u in Section 2).

3.1. The state equation. As mentioned in the previous section we replace the p-Laplace equation in the optimization by a simpler (i.e., linear) elliptic PDE. For given (positive) thickness parameter $\mu : \Omega \to \mathbb{R}$ and force term $g : \Omega \to \mathbb{R}$ we assume that the displacement of the material is governed by the solution $v : \Omega \to \mathbb{R}$ to the linear, elliptic PDE

$$-\operatorname{div}\big(2(1+n)\mu(\mathbf{x})\nabla v(\mathbf{x})\big) = g(\mathbf{x}) \qquad \text{for all } \mathbf{x} \in \Omega, \tag{3.1a}$$

$$v(\mathbf{x}) = 0 \qquad \text{for all } \mathbf{x} \in \Gamma. \tag{3.1b}$$

A weak solution to (3.1) is defined as follows: If $v \in V$ holds and v satisfies

$$\int_\Omega 2(1+n)\mu(\mathbf{x})\nabla v(\mathbf{x}) \cdot \nabla\varphi(\mathbf{x})\,\mathrm{d}\mathbf{x} = \langle g, \varphi\rangle_{V',V} \quad \text{for all } \varphi \in V,$$

then v is called a *weak solution to* (3.1). Here, $\langle\cdot\,,\cdot\rangle_{V',V}$ denotes the dual pairing between V and its dual space V'.

Proposition 3.1. *Let $g \in V'$. If $\mu \in L^\infty(\Omega)$ satisfies $\mu(\mathbf{x}) \geq \mu_a$ f.a.a. $\mathbf{x} \in \Omega$ with a positive scalar μ_a, then* (3.1) *possesses a unique weak solution v satisfying*

$$\|v\|_V \leq C\|g\|_{V'} \tag{3.2}$$

with a constant $C \geq 0$ depending on the Hollomon coefficient n and on μ_a, but not on μ. If, in addition, Ω is convex, Γ is Lipschitz-continuous, μ lies in $C^{0,1}(\overline{\Omega})$ (the space of all Lipschitz-continuous functions on $\overline{\Omega}$) and $g \in L^2(\Omega)$, then $v \in H^2(\Omega) \cap V$ holds.

Proof. The existence of a unique weak solution follows from the Lax-Milgram theorem [11, p. 297]. The proof of estimate (3.2) follows from standard variational techniques. For the regularity result we refer to [21, p. 132]. □

Remark 3.2.
1) It follows from Proposition 3.1, $\Omega \subset \mathbb{R}^2$ and the Sobolev embedding theorem (see, e.g., [1]) that $v \in C(\overline{\Omega})$ holds.
2) Recall that the Hilbert space $H^s(\Omega) \cap V$ is compactly embedded into $C(\overline{\Omega})$ and into $H_0^1(\Omega)$ for $s > \max(1, d/2)$; see, e.g., [1]. ◊

Next we write the PDE as an operator equation. For that purpose let us define the Banach space $Y = L^\infty(\Omega) \times V$ endowed with the natural product topology

$$\|y\|_Y = \|\mu\|_{L^\infty(\Omega)} + \|v\|_V \quad \text{for } y = (\mu, v) \in Y.$$

Moreover, we introduce the bilinear operator $c : Y \to V'$ by

$$\langle c(y), \varphi\rangle_{V',V} = \int_\Omega 2(1+n)\mu(\mathbf{x})\nabla v(\mathbf{x}) \cdot \nabla\varphi(\mathbf{x})\,\mathrm{d}\mathbf{x} - \langle g, \varphi\rangle_{V',V}$$

for $y = (\mu, v) \in Y$ and $\varphi \in V$.

Remark 3.3. a) Let $y = (\mu, v)$ satisfy $c(y) = 0$ and $\mu(\mathbf{x}) \geq \mu_a > 0$ f.a.a. $\mathbf{x} \in \Omega$. Then, v is a weak solution to (3.1). On the other hand, if v is a weak solution to (3.1) for given $\mu \in M_{ad}$, then $c(y) = 0$.

b) Associated with the fine model $f(x) = 0$ for $x = (\lambda, u) \in X$ in Section 2.4 (accurate, but expensive) we consider now the coarse model $c(y) = 0$ for $y = (\mu, v) \in Y$, which is less accurate but computationally cheaper. ◊

The proof of the following lemma is given in the Appendix.

Lemma 3.4. *For every $y = (\mu, v) \in Y$ the operator $c : Y \to V'$ is twice continuously Fréchet-differentiable and its Fréchet derivatives are given by*

$$\langle c'(y)y_\delta, \varphi\rangle_{V',V} = \int_\Omega 2(1+n)\big(\mu_\delta(\mathbf{x})\nabla v(\mathbf{x}) + \mu(\mathbf{x})\nabla v_\delta(\mathbf{x})\big)\cdot\nabla\varphi(\mathbf{x})\,\mathrm{d}\mathbf{x}, \tag{3.3}$$

$$\begin{aligned}&\langle c''(y)(y_\delta, \tilde{y}_\delta), \varphi\rangle_{V',V}\\ &\qquad = \int_\Omega 2(1+n)\big(\mu_\delta(\mathbf{x})\nabla\tilde{v}_\delta(\mathbf{x}) + \tilde{\mu}_\delta(\mathbf{x})\nabla v_\delta(\mathbf{x})\big)\cdot\nabla\varphi(\mathbf{x})\,\mathrm{d}\mathbf{x}\end{aligned} \tag{3.4}$$

for any directions $y_\delta = (\mu_\delta, v_\delta)$, $\tilde{y}_\delta = (\tilde{\mu}_\delta, \tilde{v}_\delta) \in Y$ and for $\varphi \in V$.

The following proposition will be used in Section 3.3 to ensure the existence of a Lagrange multiplier (or a dual variable). For the proof we refer to the Appendix.

Proposition 3.5. *Let $y = (\mu, v) \in Y$ satisfy $\mu(\mathbf{x}) \geq \mu_a$ f.a.a. $\mathbf{x} \in \Omega$ with a positive scalar μ_a, then the partial Fréchet derivative $c_v(y) : V \to V'$ of c with respect to v at y is bijective.*

Remark 3.6. Let $y = (\mu, v) \in Y$ satisfy $\mu(\mathbf{x}) \geq \mu_a$ f.a.a. $\mathbf{x} \in \Omega$ with a positive scalar μ_a. By Proposition 3.5 the first Fréchet derivative

$$c'(y) = (c_\mu(y), c_v(y)) : Y \to V'$$

is a surjective operator. In particular, $y_\delta = (\mu_\delta, v_\delta) \in \ker c'(y)$ if and only if

$$c'(y)y_\delta = 0 \quad \text{in } V',$$

which is equivalent with the fact that y_δ satisfies the variational problem

$$\int_\Omega 2(1+n)\big(\mu(\mathbf{x})\nabla v_\delta(\mathbf{x}) + \mu_\delta(\mathbf{x})\nabla v(\mathbf{x})\big)\cdot\nabla\varphi(\mathbf{x})\,\mathrm{d}\mathbf{x} = 0 \quad \text{for all } \varphi \in V. \tag{3.5}$$

Choosing $\varphi = v_\delta$ we infer from (3.5) that

$$2(1+n)\mu_a \|v_\delta\|_V^2 \leq 2(1+n)\|\mu_\delta\|_{L^\infty}\|v\|_V\|v_\delta\|_V.$$

Consequently,

$$\|v_\delta\|_V \leq C\,\|\mu_\delta\|_{L^\infty(\Omega)},$$

where the constant $C > 0$ depends on μ_a and $\|v\|_V$, but not on μ_δ. ◊

3.2. Numerical comparison with the *p*-Laplace equation. Next we compare the numerical weak solution v to (3.1) to the corresponding one u to (2.2). For that purpose we choose the thickness parameters $\mu = \lambda$ as in Section 2.2; see left plots of Figures 2.1 and 2.2. The FE discretization is also the same as in Section 2.2. Furthermore, the Hollomon coefficient is set to $n = 0.22$ and ε is 10^{-10}. Then, the numerical solution u for $\mu = 0.75$ is shown in Figure 3.1 (left plot). The absolute difference between v and the corresponding solution of the p-Laplace equation is shown in the right plot of Figure 3.1. Now we choose the structured thickness

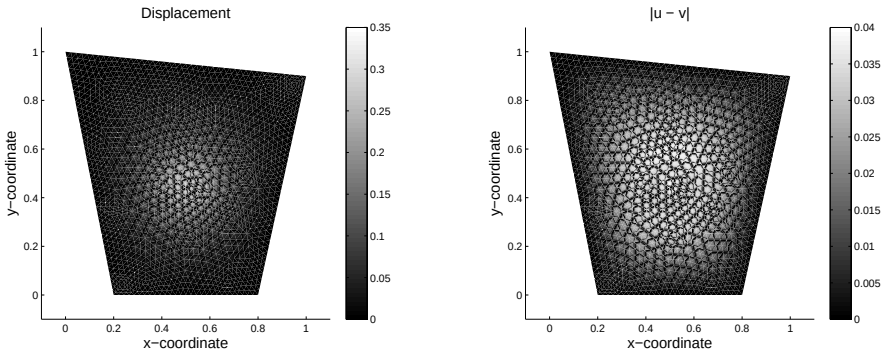

FIGURE 3.1. Weak solution v to (3.1) for the constant thickness parameter plotted in left plot of Figure 2.1 (left plot) and difference $|u-v|$, where u is the corresponding weak solution to the p-Laplace equation (right plot).

parameter as plotted in Figure 2.2 (left plot). The numerical solution v to (3.1) is plotted in Figure 3.2 (left plot), whereas the absolute differenz between v and the corresponding solution of the p-Laplace equation is shown in Figure 3.2 (right plot). When looking at Figures 3.1 and 3.2, one can see the different behaviours of the

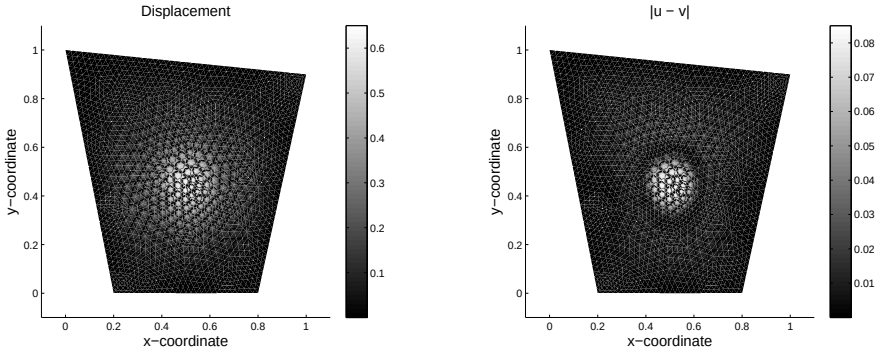

FIGURE 3.2. Weak solution v to (3.1) for the non-constant thickness parameter plotted in left plot of Figure 2.2 (left plot) and difference $|u-v|$, where u is the corresponding weak solution to the p-Laplace equation (right plot).

non-linear and the linear problems; see also Table 3.1 for values of different norms. We observe from Table 3.1 that for the constant thickness parameter the maximal displacement obtained from the p-Laplace equation is larger than the corresponding one derived from the linear PDE. On the other hand, the situation is different for our non-constant thickness parameter.

3.3. The optimal control problem. The goal is to determine an optimal thickness parameter μ and a corresponding optimal displacement v minimizing the cost

Thickness	$\|u-v\|_{L^2(\Omega)}$	$\max_\Omega u$	$\max_\Omega v$
constant $\lambda=\mu$	0.0177	0.3026	0.2633
non-constant $\lambda=\mu$	0.0148	0.5389	0.6205

TABLE 3.1. Comparison of the non-linear (u) and the linear (v) weak solutions for two different choices of thickness parameter.

functional $\mathcal{J}: Y \to \mathbb{R}$ given by

$$\mathcal{J}(\mu,v) = \int_\Omega \mu(\mathbf{x}) + \frac{\eta}{2}\left|\mu-\mu^\circ(\mathbf{x})\right|^2 + \beta\,\Phi\big(v(\mathbf{x})-v_b(\mathbf{x})\big)\,\mathrm{d}\mathbf{x}$$

for $y=(\mu,v)\in Y$ subject to the equality constraints $c(y)=0$ in V' and to the inequality constraints

$$\mu_a \le \mu(\mathbf{x}) \le \mu_b \quad \text{f.a.a. } \mathbf{x}\in\Omega,$$

where μ_a, μ_b are positive scalars with $\mu_a \le \mu_b$. Furthermore, η, β are as in Section 2.3 and $v_b \in L^2(\Omega)$ satisfies $v_b(\mathbf{x}) \ge 0$ f.a.a. $\mathbf{x}\in\Omega$.

The next result is proved in the Appendix.

Lemma 3.7. *Suppose that $\Phi \in C^2(\mathbb{R})$. Then, for every $y=(\mu,v)\in Y$ the cost functional $\mathcal{J}$ is twice continuously Fréchet-differentiable. The Fréchet derivatives are given by*

$$\mathcal{J}'(y)y_\delta = \int_\Omega \mu_\delta(\mathbf{x}) + \eta\,\big(\mu(\mathbf{x})-\mu^\circ(\mathbf{x})\big)v_\delta(\mathbf{x}) + \beta\,\Phi'\big(v(\cdot)-v_b(\cdot)\big)v_\delta(\mathbf{x})\,\mathrm{d}\mathbf{x},$$

$$\mathcal{J}''(y)(y_\delta,\tilde{y}_\delta) = \int_\Omega \eta\mu_\delta(\mathbf{x})\tilde{\mu}_\delta(\mathbf{x}) + \beta\,\Phi''\big(v(\cdot)-v_b(\cdot)\big)v_\delta(\mathbf{x})\tilde{v}_\delta(\mathbf{x})\,\mathrm{d}\mathbf{x}$$

for any direction $y_\delta=(\mu_\delta,v_\delta)$, $\tilde{y}_\delta=(\tilde{\mu}_\delta,\tilde{v}_\delta)\in Y$.

We introduce the set of admissible thickness parameters by

$$M_{ad} = \big\{\mu\in L^2(\Omega)\,\big|\,\mu_a\le\mu(\mathbf{x})\le\mu_b \text{ f.a.a. } \mathbf{x}\in\Omega\big\}$$

and define $Y_{ad}=M_{ad}\times V$. Moreover, the set of admissible solutions is

$$\mathcal{F}(\mathbf{P}_c) = \big\{y\in Y_{ad}\,\big|\,c(y)=0 \text{ in } V'\big\}.$$

Now the minimization problem can be formulated abstractly as

$$\min \mathcal{J}(y) \quad \text{s.t.} \quad y\in\mathcal{F}(\mathbf{P}_c). \tag{$\mathbf{P}_c$}$$

To ensure existence of an optimal solution to ($\mathbf{P}_c$) we have to ensure the following assumption. Recall that by Proposition 3.1 there exists a unique $v\in V$ solving $c(\mu,v)=0$ in V' for any $\mu\in M_{ad}$.

Assumption 1. 1) *Suppose that $\Phi\in C^2(\mathbb{R})$ is weakly lower semi-continuous.*
2) *For every $\mu\in M_{ad}$ the unique weak solution v to (3.1) lies in the Hilbert space $H^s(\Omega)$ with $s>\max(1,d/2)$ and*

$$\|v\|_{H^s(\Omega)} \le C\big(1+\|\mu\|_{L^\infty(\Omega)}\big)$$

for a constant $C>0$.

The next theorem ensures that ($\mathbf{P}_c$) has a local solution. The proof is given in the Appendix.

Theorem 3.8. *Let Assumption* 1 *hold. Then,* $(\mathbf{P}_c)$ *has at least one optimal solution.*

Remark 3.9. Assumption 1 can be avoided provided we enforce the parameter λ to lie in a smoother space, e.g., in the Hölder space $C^{0,1}(\overline{\Omega})$; see Proposition 3.1. However, motivated by our application we would not like to require more regularity for the thickness parameter μ; see, e.g., the example in Figure 2.2, left plot. $\Diamond$

3.4. First-order optimality conditions. Let $y^* = (\mu^*, v^*) \in Y_{ad}$ be a (local) optimal solution to $(\mathbf{P}_c)$. Then, x^* can be characterized by *first-order necessary optimality conditions* [17]. For that purpose we introduce the Lagrange functional $L : Y \times V \to \mathbb{R}$ by

$$\begin{aligned} L(y,p) &= \mathcal{J}(y) + \langle c(y), p\rangle_{V',V} \\ &= \int_\Omega \mu(\mathbf{x}) + \eta\big(\mu(\mathbf{x}) - \mu^\circ(\mathbf{x})\big) + \beta\Phi\big(v(\mathbf{x}) - v_b(\mathbf{x})\big) \\ &\quad + \int_\Omega 2(1+n)\mu(\mathbf{x})\nabla v(\mathbf{x})\cdot\nabla p(\mathbf{x})\,\mathrm{d}\mathbf{x} - \langle g, p\rangle_{V',V} \end{aligned}$$

for $y = (\mu, v) \in Y$ and $p \in V$. Due to Lemmas 3.4 and 3.7 the Lagrangian is Fréchet-differentiable. At a given point $(y,p) \in Y \times V$ we obtain

$$\begin{aligned} \nabla L(y,p)(y_\delta, p_\delta) = &\int_\Omega \mu_\delta(\mathbf{x}) + \eta\left(\mu(\mathbf{x}) - \mu^\circ(\mathbf{x})\right)v_\delta(\mathbf{x})\,\mathrm{d}\mathbf{x} \\ &+ \int_\Omega \beta\Phi'\big(v(\mathbf{x}) - v_b(\mathbf{x})\big)v_\delta(\mathbf{x})\,\mathrm{d}\mathbf{x} \\ &+ \int_\Omega 2(1+n)\Big(\big(\mu(\mathbf{x})\nabla v_\delta(\mathbf{x}) + \mu_\delta(\mathbf{x})\nabla v(\mathbf{x})\big)\cdot\nabla p(\mathbf{x})\Big)\,\mathrm{d}\mathbf{x} \\ &+ \int_\Omega 2(1+n)\mu(\mathbf{x})\nabla v(\mathbf{x})\cdot\nabla p_\delta(\mathbf{x})\,\mathrm{d}\mathbf{x} - \langle g, p_\delta\rangle_{V',V} \end{aligned} \tag{3.6}$$

for any directions $y_\delta = (\mu_\delta, v_\delta) \in Y$ and $p_\delta \in V$. The gradient of the Lagrange functional is the basis for the first-order necessary optimality conditions for $(\mathbf{P}_c)$. These optimality conditions are formulated in the next theorem, which is proved in the Appendix.

Theorem 3.10. *Let Assumption* 1 *hold. Suppose that* $y^* = (\mu^*, v^*)$ *is a local solution to* $(\mathbf{P}_c)$. *Then there exists a unique associated Lagrange multiplier* $p^* \in V$ *satisfying together with* y^* *the* dual *or* adjoint equations

$$-\mathrm{div}\left(2(1+n)\mu^*(\mathbf{x})\nabla p^*(\mathbf{x})\right) = -\beta\Phi'\big(v^*(\mathbf{x}) - v_b(\mathbf{x})\big) \qquad \textit{f.a.a. } \mathbf{x}\in\Omega, \tag{3.7a}$$

$$p^*(\mathbf{x}) = 0 \qquad \textit{f.a.a. } \mathbf{x}\in\Gamma. \tag{3.7b}$$

Moreover, the variational inequality

$$\int_\Omega \Big(1+\eta\left(\mu^*(\mathbf{x})-\mu^\circ(\mathbf{x})\right)+2(1+n)\nabla v^*(\mathbf{x})\cdot\nabla p^*(\mathbf{x})\Big)\left(\mu_\delta(\mathbf{x})-\mu^*(\mathbf{x})\right)\mathrm{d}\mathbf{x} \geq 0 \tag{3.8}$$

for all $\mu_\delta \in M_{ad}$ *holds.*

Remark 3.11. The first-order necessary optimality conditions can be summerized as follows: Suppose that $y^* = (\mu^*, v^*) \in \mathcal{F}(\mathbf{P}_c)$ is a local solution to $(\mathbf{P}_c)$. Then,

there exists a unique associated Lagrange multiplier $p^* \in V$ solving together with $y^* = (\mu^*, v) \in Y_{ad}$

$$\begin{aligned}
-\operatorname{div}\big(2(1+n)\mu^*(\mathbf{x})\nabla v^*(\mathbf{x})\big) &= g(\mathbf{x}) && \text{f.a.a. } \mathbf{x} \in \Omega,\\
v^*(\mathbf{x}) &= 0 && \text{f.a.a. } \mathbf{x} \in \Gamma,\\
-\operatorname{div}\big(2(1+n)\mu^*(\mathbf{x})\nabla p^*(\mathbf{x})\big) &= -\beta\Phi'\big(v^*(\mathbf{x}) - v_b(\mathbf{x})\big) && \text{f.a.a. } \mathbf{x} \in \Omega,\\
p^*(\mathbf{x}) &= 0 && \text{f.a.a. } \mathbf{x} \in \Gamma,
\end{aligned} \tag{3.9}$$

$$\int_\Omega \Big(1 + \eta\big(\mu^*(\mathbf{x}) - \mu^\circ(\mathbf{x})\big) + 2(1+n)\nabla v^*(\mathbf{x})\cdot\nabla p^*(\mathbf{x})\Big) \cdot \big(\mu_\delta(\mathbf{x}) - \mu^*(\mathbf{x})\big)\,\mathrm{d}\mathbf{x} \geq 0$$

for all $\mu_\delta \in M_{ad}$. ◊

3.5. The reduced problem. Let Assumption 1 hold. Due to Proposition 3.1 there exists a unique weak solution $v = v(\mu) \in H^s(\Omega) \cap V$ for any $\mu \in M_{ad}$. Therefore, we introduce the solution operator $\mathcal{S} : T_{ad} \to V$ so that $v(\mu) = \mathcal{S}(\mu)$ for $\mu \in M_{ad}$. Let us mention that $c(\mu, \mathcal{S}(\mu)) = 0$ for any $\mu \in M_{ad}$. Now, we define the reduced cost functional $\hat{\mathcal{J}} : M_{ad} \to \mathbb{R}$ by

$$\hat{\mathcal{J}}(\mu) = \mathcal{J}(\mu, \mathcal{S}(\mu)) \quad \text{for } \mu \in M_{ad}$$

and consider the reduced optimal control problem

$$\min \hat{\mathcal{J}}(\mu) \quad \text{s.t.} \quad \mu \in M_{ad}. \tag{$\hat{\mathbf{P}}_c$}$$

Compared to ($\mathbf{P}_c$) the reduced problem ($\hat{\mathbf{P}}_c$) has no explicit equality constraints. Let $y^* = (\mu^*, v^*)$ be a solution to ($\mathbf{P}_c$). Then, $v^* = \mathcal{S}(\mu^*)$ holds. Thus, μ^* solves ($\hat{\mathbf{P}}_c$). Vice versa, if μ^* is a solution to ($\hat{\mathbf{P}}_c$), then $y^* = (\mu^*, \mathcal{S}(\mu^*))$ solves ($\mathbf{P}_c$).

The gradient of the reduced cost functional at a given point $\mu \in M_{ad}$ in a direction $\mu_\delta \in L^\infty(\Omega)$ is given by

$$\hat{\mathcal{J}}'(\mu)\mu_\delta = \int_\Omega \Big(1 + \eta\big(\mu(\mathbf{x}) - \mu^\circ(\mathbf{x})\big) + 2(1+n)\nabla v(\mathbf{x})\cdot\nabla p(\mathbf{x})\Big)\mu_\delta(\mathbf{x})\,\mathrm{d}\mathbf{x},$$

where v satisfies (3.1) and p solves

$$\begin{aligned}
-\operatorname{div}\big(2(1+n)\mu(\mathbf{x})\nabla p(\mathbf{x})\big) &= -\beta\Phi'\big(v(\mathbf{x}) - v_b(\mathbf{x})\big) && \text{f.a.a. } \mathbf{x} \in \Omega,\\
p(\mathbf{x}) &= 0 && \text{f.a.a. } \mathbf{x} \in \Gamma.
\end{aligned} \tag{3.10}$$

3.6. Second-order optimality conditions. Let $y^* = (\mu^*, v^*) \in Y_{ad}$ be a local solution to ($\mathbf{P}_c$) satisfying $\mu_a < \mu < \mu_b$ in Ω a.e. (i.e., the optimal solution is an inactive solution). Furthermore, $p^* \in V$ is the associated Lagrange multiplier. Using Lemmas 3.4 and 3.7 we find

$$\begin{aligned}
L_{yy}(y,p)\big(y_\delta, y_\delta\big) = &\int_\Omega \eta\mu_\delta(\mathbf{x})^2 + \beta\Phi''\big(v(\mathbf{x}) - v_b(\mathbf{x})\big)v_\delta(\mathbf{x})^2\,\mathrm{d}\mathbf{x}\\
&+ \int_\Omega 4(1+n)\mu_\delta(\mathbf{x})\nabla v_\delta(\mathbf{x})\cdot\nabla p(\mathbf{x})\,\mathrm{d}\mathbf{x}
\end{aligned}$$

at $y = (\mu, v) \in Y$, $p \in V$ and in a direction $y_\delta = (\mu_\delta, v_\delta) \in Y$. Thus, it is not a-priorily clear that the second-order sufficient optimality condition holds, i.e.,

$$L_{yy}(y^*, p^*)\big(y_\delta, y_\delta\big) \geq \sigma \|y_\delta\|_Y^2 \quad \text{for all } y_\delta \in \ker c'(y^*) \tag{3.11}$$

and for a constant $\sigma > 0$. For this reason we assume the following hypothesis.

Assumption 2. *Problem* $(\hat{\mathbf{P}}_c)$ *has a local solution* $\mu^* \in L^\infty(\Omega)$ *satisfying* $\mu_a < \mu^*(\mathbf{x}) < \mu_b$ *f.a.a.* $\mathbf{x} \in \Omega$. *Let* $v^* = \mathcal{S}(\mu^*) \in H^s(\Omega)$, $s > \max(1, d/2)$, *be the corresponding optimal state and* $p^* \in H^s(\Omega) \cap V$ *the associated Lagrange multiplier. Then, there exists a constant* $\sigma > 0$ *so that the second-order sufficient optimality condition* (3.11) *is satisfied.*

Remark 3.12. In our numerical experiments we choose $\Phi(s) = \max(s, 0)^3/3$. Thus, $\Phi''(s) \geq 0$ for all $s \in \mathbb{R}$. However, (3.11) can not be ensured without assumptions on the dual variable p^*. $\Diamond$

3.7. Numerical examples. In this subsection we present numerical test examples for $(\hat{\mathbf{P}}_c)$. Assuming Assumption 2 we utilize a globalized Newton method, which for the readers convenience is repeated in Algorithm 1. For a convergence analysis we refer, e.g., to [18].

Algorithm 1 (Globalized Newton method)

1: Choose a starting value $\mu^0 \in M_{ad}$, a tolerance $\varepsilon > 0$ and set $k = 0$.
2: **repeat**
3: Compute $v^k = \mathcal{S}(\mu^k)$ by solving (3.1) with $\mu = \mu^k$.
4: Set $\mu = \mu^k$, $v = v^k$, and solve (3.10) for $p = p^k$ and determine $\hat{\mathcal{J}}'(\mu^k)$.
5: Solve for $\mu_\delta \in L^\infty(\Omega)$ the Newton system

$$\hat{\mathcal{J}}''(\mu^k)\mu_\delta = -\hat{\mathcal{J}}'(\mu^k) \tag{3.12}$$

utilizing the truncated conjugate gradient method; see, e.g., [18, p. 169].
6: Determine a step length parameter $s_k \in (0, 1]$ by Armijo backtracking.
7: Set $\mu^{k+1} = \mu^k + s_k\mu_\delta \in M_{ad}$ and $k = k + 1$.
8: **until** some stopping criterium is satisfied.

Remark 3.13. a) System (3.12) is solved by the conjugate gradient (CG) method. The application of the hessian $\hat{\mathcal{J}}''(\mu^k)$ is given by

$$\big(\hat{\mathcal{J}}''(\mu^k)\mu_\delta^k\big)(\mathbf{x}) = \eta v_\delta(\mathbf{x}) + 2(1+n)\big(\nabla v^k(\mathbf{x}) \cdot \nabla p_\delta(\mathbf{x}) + \nabla v_\delta(\mathbf{x}) \cdot \nabla p^k(\mathbf{x})\big)$$

for any direction $\mu_\delta \in L^\infty(\Omega)$ and f.a.a. $\mathbf{x} \in \Omega$, where

$$\begin{aligned}
-\operatorname{div}\big(2(1+n)\mu^k(\mathbf{x})\nabla v_\delta(\mathbf{x})\big) &= \operatorname{div}\big(2(1+n)\mu_\delta(\mathbf{x})\nabla v^k(\mathbf{x})\big) && \text{f.a.a. } \mathbf{x} \in \Omega,\\
v_\delta(\mathbf{x}) &= 0 && \text{f.a.a. } \mathbf{x} \in \Gamma,\\
-\operatorname{div}\big(2(1+n)\mu^k(\mathbf{x})\nabla p_\delta(\mathbf{x})\big) &= \operatorname{div}\big(2(1+n)\mu_\delta(\mathbf{x})\nabla p^k(\mathbf{x})\big)\\
&\quad - \beta\Phi''\big(v^k(\mathbf{x}) - v_b(\mathbf{x})\big)v_\delta(\mathbf{x}) && \text{f.a.a. } \mathbf{x} \in \Omega,\\
p_\delta(\mathbf{x}) &= 0 && \text{f.a.a. } \mathbf{x} \in \Gamma.
\end{aligned}$$

b) We can not guarantee that $\hat{\mathcal{J}}''(\mu^k)$ is a coercive operator for all $k \geq 0$. Therefore, we apply the truncated CG method [18, p. 169]. If negative curvature is detected on the first CG iteration, the returned direction is the steepest descent direction. If negative curvature occurs on the j-th CG iteration with $j > 1$ then the CG direction of the $(j-1)$-th CG iteration is the returned CG direction. In both cases the returned CG directions are descent directions.

k	$\hat{\mathcal{J}}(\mu^k)$	$\frac{\eta}{2}\|\mu^k - \mu^\circ\|^2_{L^2(\Omega)}$	$\|\hat{\mathcal{J}}'(\mu^k)\|_{L^2(\Omega)}$	$\langle \hat{\mathcal{J}}'(\mu^k), \mu_\delta \rangle_{L^2(\Omega)}$
0	2.1936	0.0297	61.80878	—
1	1.1031	0.0256	21.72930	−1.7327
2	0.7614	0.0224	7.23516	−0.5505
3	0.6702	0.0205	2.26640	−0.1491
4	0.6497	0.0197	0.69051	−0.0342
5	0.6212	0.0644	1.46964	−0.0651
6	0.6103	0.0627	0.36406	−0.0188
7	0.6031	0.0882	0.13905	−0.0136
8	0.6025	0.0901	0.02111	−0.0009
9	0.6025	0.0929	0.00078	−0.0001

TABLE 3.2. Run 3.1: Convergence results for Algorithm 1 using an initial thickness parameter of $\mu^0 = 0.75$.

c) In the Armijo backtracking line search (see step 6 of Algorithm 1) is based on the Armijo rule

$$\hat{J}(\mu^k + s\mu_\delta) \leq \hat{J}(\mu^k) + cs\langle \hat{J}'(\mu^k), \mu_\delta \rangle_{L^2(\Omega)} \tag{3.13}$$

with $c \in (0,1)$. If (3.13) holds, we set $s_k = s$. Otherwise, we test (3.13) with $s = s/2$.

d) The stopping criterium in step 8 of Algorithm 1 is chosen as follows

$$\|\hat{\mathcal{J}}'(\mu^k)\|_{L^2(\Omega)} \leq \varepsilon_{rel} \|\hat{\mathcal{J}}'(\mu^0)\|_{L^2(\Omega)} + \varepsilon_{abs}$$

with a relative tolerance $\varepsilon_{rel} > 0$ and an absolute tolerance $\varepsilon_{abs} \geq \varepsilon_{rel}$. ◊

Run 3.1. We utilize the two-dimensional domain Ω and the same discretization as in Sections 2.2 and 3.2. Moreover, the force g and the Hollomon coefficient n are as in Section 2.2. Let $v_b = 0.2$, $\beta = 25 \cdot 10^5$, $\mu^\circ = 1$, and $\eta = 1.25$. As initial thickness we use $\mu^0 = 0.75$. We implement Algorithm 1 and solve the Newton step by the truncated CG method. The relative and absolute tolerances are $\varepsilon_{rel} = 10^{-4}$ and $\varepsilon_{abs} = 10^{-6}$, respectively. We start Algorithm 1 with $\mu^0 = 0.75$. The method stops after 21 seconds. In Table 3.2 the convergence performance is presented. The optimal solution is plotted in Figure 3.3. ◊

4. Space mapping techniques

The space mapping is a mapping between the fine-model space of parameters or variables and the coarse model space so that the optimization can be carried out for the coarse model, but information from the fine model is utilized to improve the accuracy of the optimization result with respect to the real application.

4.1. The space mapping. The optimal control problem $(\hat{\mathbf{P}}_f)$ is governed by the quasilinear PDE (2.2) that includes non-linear effects of the material, but is expensive to solve. On the other hand, $(\hat{\mathbf{P}}_f)$ is relatively cheap, but not as accurate as $(\hat{\mathbf{P}}_f)$. To combine the advantage of the simpler optimal control problem $(\hat{\mathbf{P}}_f)$ with the advantage of the more realistic model (3.1) we introduce a space mapping.

For $\mathcal{A} \subseteq \Omega$ we define the restriction operator $\mathcal{R}_\mathcal{A} : L^2(\Omega) \to L^2(\Omega)$ as

$$\mathcal{R}_\mathcal{A} v = v \text{ on } \mathcal{A} \text{ a.e.} \quad \text{and} \quad \mathcal{R}_\mathcal{A} v = 0 \text{ otherwise.}$$

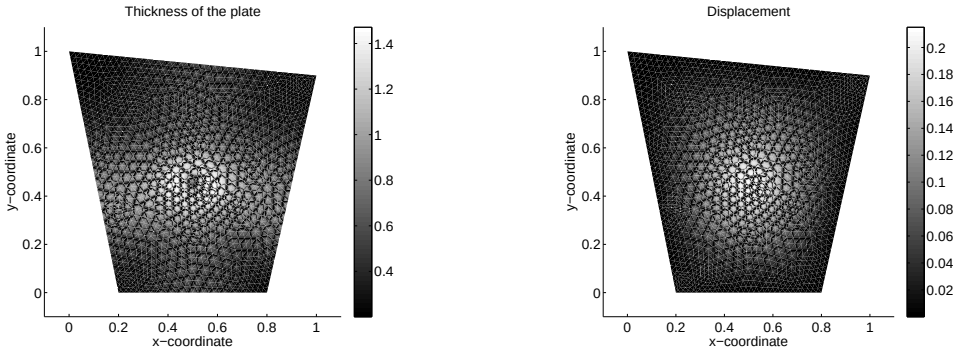

FIGURE 3.3. Run 3.1: Optimal thickness parameter (left plot) and the optimal displacement (right plot) for an initial thickness parameter of $\mu^0 = 0.75$.

Now we introduce the space mapping $\mathcal{P} : \Lambda_{ad} \to M_{ad}$ as follows: for given $\lambda \in \Lambda_{ad}$ the thickness parameter $\mu = \mathcal{P}(\lambda) \in M_{ad}$ is the thickness parameter so that $\mathcal{R}_{\mathcal{A}} v$ is as close to $\mathcal{R}_{\mathcal{A}} u$, where $v = \mathcal{S}(\mathcal{P}(\lambda))$ and $u = S(\lambda)$ hold. We formulate μ as the solution to a minimization problem: $\mu = \mathcal{P}(\lambda)$ is the solution to

$$\begin{aligned} &\min \hat{J}_{sp}(\mu) = \frac{\gamma}{2} \int_{\mathcal{A}} \big|\mathcal{S}(\mu)(\mathbf{x}) - u(\mathbf{x})\big|^2 \,\mathrm{d}\mathbf{x} + \frac{\kappa}{2} \int_{\Omega} \big|\mu(\mathbf{x}) - \lambda(\mathbf{x})\big|^2 \,\mathrm{d}\mathbf{x} \\ &\text{s.t.} \quad \mu \in M_{ad}, \end{aligned} \tag{$\mathbf{P}_{sp}$}$$

where $\gamma > 0$ is weighting parameters and $\kappa \geq 0$ is a smoothing parameter.

Note that $(\mathbf{P}_{sp})$ may have no or more than one solution. Thus, we suppose that there exists at least one optimal solution $\mu_* \in M_{ad}$ to $(\mathbf{P}_{sp})$. For more details we refer to [14]. Using the Lagrangian approach, the first-order necessary optimality conditions for $(\mathbf{P}_{sp})$ are given as

$$\int_{\Omega} \big(\kappa\big(\mu_*(\mathbf{x}) - \lambda(\mathbf{x})\big) + 2(1+n)\big(\nabla v_*(\mathbf{x}) \cdot \nabla p_*(\mathbf{x})\big)\big)\,\big(\mu_\delta(\mathbf{x}) - \mu_*(\mathbf{x})\big)\,\mathrm{d}\mathbf{x} \geq 0 \tag{4.1}$$

for all $\mu_\delta \in M_{ad}$, where $v_* = \mathcal{S}(\mu_*)$ holds and p_* is the weak solution to

$$\begin{aligned} -\mathrm{div}\,\big(2(1+n)\mu_*(\mathbf{x})\nabla p_*(\mathbf{x})\big) &= -\gamma\big(\mathcal{R}_{\mathcal{A}}(v_* - u)\big)(\mathbf{x}) \qquad &&\text{f.a.a. } \mathbf{x} \in \Omega, \\ p_*(\mathbf{x}) &= 0 \qquad &&\text{f.a.a. } \mathbf{x} \in \Gamma. \end{aligned}$$

In particular, the gradient $\hat{J}'_{sp}$ at a value μ reads

$$\hat{J}'_{sp}(\mu) = 2(1+n)\big(\nabla v(\cdot) \cdot \nabla p(\cdot)\big) + \kappa\big(\mu(\cdot) - \lambda(\cdot)\big),$$

where $v = \mathcal{S}(\mu)$ holds and p is the weak solution to

$$\begin{aligned} -\mathrm{div}\,\big(2(1+n)\mu(\mathbf{x})\nabla p(\mathbf{x})\big) &= -\gamma\big(\mathcal{R}_{\mathcal{A}}(v - u)\big)(\mathbf{x}) \qquad &&\text{f.a.a. } \mathbf{x} \in \Omega, \\ p(\mathbf{x}) &= 0 \qquad &&\text{f.a.a. } \mathbf{x} \in \Gamma. \end{aligned}$$

We assume the the solution to $(\mathbf{P}_{sp})$ is an inactive solution.

Assumption 3. *Problem* $(\mathbf{P}_{sp})$ *has a unique solution* μ_* *satisfying* $\mu_a < \mu_* < \mu_b$ *f.a.a.* $\mathbf{x} \in \Omega$.

Remark 4.1. If Assumption 3 holds, the first-order necessary optimality conditions for $(\mathbf{P}_{sp})$ are given by

$$\langle \hat{J}'_{sp}(\mu_*), \mu_\delta \rangle_{L^2(\Omega)} = 0 \quad \text{for all } \mu_\delta \in L^\infty(\Omega).$$

or, equivalently,

$$2(1+n)\big(\nabla v_*(\cdot)\cdot\nabla p_*(\cdot)\big) + \kappa\big(\mu_*(\cdot) - \lambda(\cdot)\big) = 0, \tag{4.2}$$

that is a non-linear equation. ◊

We utilize a globalized Newton method to solve (4.2). For the readers convenience, the method is stated in Algorithm 2.

Algorithm 2 (Newton method for computing the space mapping)

1: Choose initial $\mu^0 \in L^\infty(\Omega)$ and set $\ell = 0$.
2: **repeat**
3: Solve for $\mu_\delta \in L^\infty(\Omega)$ the linear system

$$\hat{J}''_{sp}(\mu^\ell)\mu_\delta = -\hat{J}'_{sp}(\mu^\ell) \tag{4.3}$$

utilizing the truncated CG method [18, p. 169].
4: Compute $r_\ell = \langle \hat{J}''_{sp}(\mu^\ell)\mu^\ell_\delta, \mu^\ell_\delta \rangle_{L^2(\Omega)}$.
5: Determine a step length parameter $s_\ell \in (0,1]$ by Armijo backtracking.
6: Set $\mu^{\ell+1} = \mu^\ell + s_\ell \mu_\delta$ and $\ell = \ell + 1$.
7: **until** a certain stopping criterium is fulfilled

Remark 4.2. a) To solve (4.3) by the truncated CG method $\hat{J}''_{sp}(\mu^\ell)\mu_\delta$ has to be implemented for given $\mu_\delta \in L^\infty(\Omega)$. We find

$$\big(\hat{J}''_{sp}(\mu^\ell)\mu_\delta\big)(\mathbf{x}) = \kappa\mu_\delta(\mathbf{x}) + 2(1+n)\big(\nabla v_\delta(\mathbf{x})\cdot\nabla p^\ell(\mathbf{x}) + \nabla v^\ell(\mathbf{x})\cdot\nabla p_\delta(\mathbf{x})\big)$$

f.a.a. $\mathbf{x}\in\Omega$, where v^ℓ and p^ℓ are the weak solutions to

$$\begin{aligned}
-\mathrm{div}\big(2(1+n)\mu^\ell(\mathbf{x})\nabla v^\ell(\mathbf{x})\big) &= f(\mathbf{x}) && \text{f.a.a. } \mathbf{x}\in\Omega,\\
v^\ell(\mathbf{x}) &= 0 && \text{f.a.a. } \mathbf{x}\in\Gamma,\\
-\mathrm{div}\big(2(1+n)\mu^\ell(\mathbf{x})\nabla p^\ell(\mathbf{x})\big) &= -\gamma\big(\mathcal{R}_{\mathcal{A}}(v^\ell - u)\big)(\mathbf{x}) && \text{f.a.a. } \mathbf{x}\in\Omega,\\
p^\ell(\mathbf{x}) &= 0 && \text{f.a.a. } \mathbf{x}\in\Gamma
\end{aligned}$$

and v_δ and p_δ are the weak solutions to

$$\begin{aligned}
-\mathrm{div}\big(2(1+n)\mu^\ell(\mathbf{x})\nabla v_\delta(\mathbf{x})\big) &= \mathrm{div}\big(2(1+n)\mu_\delta(\mathbf{x})\nabla v^\ell(\mathbf{x})\big) && \text{f.a.a. } \mathbf{x}\in\Omega,\\
u_\delta(\mathbf{x}) &= 0 && \text{f.a.a. } \mathbf{x}\in\Gamma,\\
-\mathrm{div}\big(2(1+n)\mu^\ell(\mathbf{x})\nabla p_\delta(\mathbf{x})\big) &= -\gamma\big(\mathcal{R}_{\mathcal{A}} v_\delta\big)(\mathbf{x})\\
&\quad + \mathrm{div}\big(2(1+n)\mu_\delta(\mathbf{x})\nabla p^\ell(\mathbf{x})\big) && \text{f.a.a. } \mathbf{x}\in\Omega,\\
p(\mathbf{x}) &= 0 && \text{f.a.a. } \mathbf{x}\in\Gamma.
\end{aligned}$$

b) Another possibility is to utilize a quasi-Newton approximation for the Hessian. Since $\hat{J}''_{sp}$ is at least positive semi-definite, a BFGS approximation is meaningful; see, e.g., [13, 18]. Using an Armijo step size algorithm, one has to check whether the BFGS matrix is positive definite or not. If the BFGS matrix is not positive definite, we use the positive definite, symmetric BFGS matrix of the previous Newton iteration. ◊

4.2. Numerical example for the space mapping. After introducing the technique of space mapping, we now report on two numerical examples. We take $\mathcal{A}$ to be a circle with radius 0.2 and mid point $(0.5, 0.45)$; compare (2.5). Our choice for the weighting parameter γ is

$$\gamma = \left(\int_\Omega \left| u(\mathbf{x}) \right|^2 \mathrm{d}\mathbf{x} \right)^{-1},$$

where u is the weak solution to (2.3) for $\epsilon = 10^{-10}$. Further we choose $\kappa = 10^{-3}\gamma$. We follow the implementation strategy described in Algorithm 2. As a stopping criteria we chose the L^2-norm of the gradient $\hat{J}'_{sp}(\mu^\ell)$ to be smaller then τ_{abs} which is given by 0.1 times the maximum triangle diameter of the discretization. To prevent an infinit loop, a maximum number of iteration is used as stopping criteria.

In our numerical experiment we compare the performance of the truncated conjugate gradient method and the BFGS method. We use two different initial thickness parameter $\lambda \in \Lambda_{ad}$.

Run 4.1. In the first example we choose the constant thickness $\lambda = 0.75$. In Figure 2.1 the thickness parameter and the solution $u = S(\lambda)$ of the p-Laplace equation are plotted. The optimal parameter μ_* solving $(\mathbf{P}_{sp})$ and the associated displacement $v_* = \mathcal{S}(\mu_*)$ are plotted in Figure 4.1. In Table 4.1 we present more details on

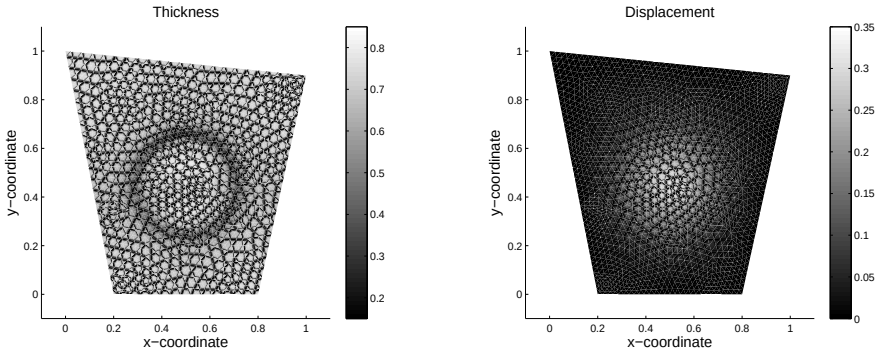

FIGURE 4.1. Run 4.1: Optimal thickness parameter μ_* (left plot) and the optimal displacement $v_* = \mathcal{S}(\mu_*)$ (right plot).

the optimization method. Here, $\hat{J}_{sp}(\mu^\ell)$ denotes the function value, $\|\hat{J}'_{sp}(\mu^\ell)\|_{L^2(\Omega)}$ the L^2-norm of the gradient and s_ℓ the step length of the line search strategy. From the fifth columns one can see that all directions are descent directions, because the directional derivative $\langle \hat{J}'_{sp}(\mu^\ell), \mu_\delta \rangle_{L^2(\Omega)}$ is negative. Next we compare the performance of the Newton-CG method with the BFGS algorithm. Since we use an Armijo backtracking line search, it is not a-priorily clear that the BFGS update formula leads to a coercive operator. If the BFGS approximation is not coercive, we use a gradient step instead of a BFGS step. The performance of the BFGS algorithm is shown in Table 4.2. When comparing Tables 4.1 and 4.2 we can see that both algorithms manage well to find a thickness parameter such that the solution of the linear model fits the solution of the non-linear model. However, the truncated CG method uses approximately 40% less iterations than the BFGS method. When comparing the CPU times, the difference is more significant. The

ℓ	$\hat{J}_{sp}(\mu^\ell)$	s_ℓ	$\|\hat{J}'_{sp}(\mu^\ell)\|_{L^2(\Omega)}$	$\langle \hat{J}'_{sp}(\mu^\ell), \mu_\delta \rangle_{L^2(\Omega)}$
0	0.0091	—	0.1763	—
1	0.0014	1.000000	0.0369	−0.0257
2	0.0013	0.015625	0.0388	−0.0457
3	0.0012	0.062500	0.0382	−0.0010
4	0.0012	0.250000	0.0360	−0.0009
5	0.0010	1.000000	0.0285	−0.0009
6	0.0006	1.000000	0.0140	−0.0006
7	0.0006	1.000000	0.0023	−0.0001

TABLE 4.1. Run 4.1: Convergence results of the Newton-CG method for the constant initial thickness.

ℓ	$\hat{J}_{sp}(\mu^\ell)$	s_ℓ	$\|\hat{J}'_{sp}(\mu^\ell)\|_{L^2(\Omega)}$	$\langle \hat{J}'_{sp}(\mu^\ell), \mu_\delta \rangle_{L^2(\Omega)}$	
0	0.0091	—	0.1763	—	
1	0.0017	0.0625	0.0510	−0.176297	GM
2	0.0015	0.0625	0.0576	−0.014769	BFGS
3	0.0014	0.1250	0.0419	−0.005786	BFGS
4	0.0010	0.2500	0.0344	−0.003047	BFGS
5	0.0009	1.0000	0.0295	−0.001484	BFGS
6	0.0007	0.2500	0.0136	−0.000998	BFGS
7	0.0006	1.0000	0.0084	−0.000191	BFGS
8	0.0006	0.5000	0.0052	−0.000091	BFGS
9	0.0006	1.0000	0.0031	−0.000015	BFGS
10	0.0006	1.0000	0.0026	−0.000009	BFGS
11	0.0006	1.0000	0.0014	−0.000010	BFGS

TABLE 4.2. Run 4.1: Convergence results of the BFGS method for the constant initial thickness. 'GM' stands for gradient step (negative curvature) and 'BFGS' means BFGS step.

truncated conjugate gradient method stops after 3.5 seconds, the BFGS method needs approximately 16 seconds. Let us mention that we also compute the space mapping by utilizing the routine `fminunc` from the MATLAB OPTIMIZATION TOOLBOX, but unfortunately the routine does not offer the possibility to integrate the corresponding norm. ◊

Run 4.2. In the second example we choose the non-constant thickness parameter λ shown in Figure 2.2 (left plot), where also the weak solution $u = S(\lambda)$ is plotted (right plot). The optimal thickness paramter μ_* and the optimal displacement $v_* = \mathcal{S}(\mu_*)$ are presented in Figure 4.2. The performance of the truncated Newton-CG and BFGS method can be seen from Tables 4.3-4.4. Again, the globalized Newton-CG method needs significantly less iterations. ◊

4.3 Surrogate Optimization. In this subsection we turn to the surrogate optimization that is used to solve approximately $(\mathbf{P}_f)$. The main idea is to solve the optimization problem using the coarse model $c(y) = 0$, but to take the fine model $f(x) = 0$ into account by the space mapping technique introduced in Section 4.2.

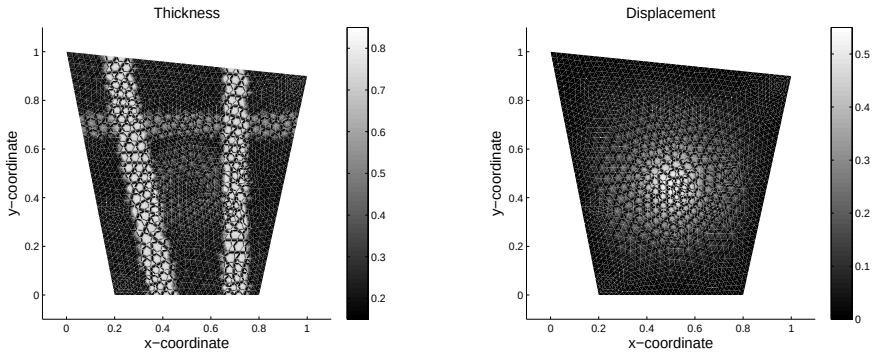

FIGURE 4.2. Run 4.2: Optimal thickness parameter μ_* (left plot) and the optimal displacement $v_* = \mathcal{S}(\mu_*)$ (right plot).

ℓ	$\hat{J}_{sp}(\mu^\ell)$	s_ℓ	$\|\hat{J}'_{sp}(\mu^\ell)\|_{L^2(\Omega)}$	$\langle \hat{J}'_{sp}(\mu^\ell), \mu_\delta \rangle_{L^2}$
0	0.00377	—	0.4452	—
1	0.00097	1.000	0.1338	−0.004422
2	0.00044	1.000	0.0476	−0.000896
3	0.00010	1.000	0.0418	−0.000887
4	0.00004	1.000	0.0040	−0.000117
5	0.00003	1.000	0.0034	−0.000017
6	0.00003	1.000	0.0003	−0.000001

TABLE 4.3. Run 4.2: Convergence results of the Newton-CG method for the non constant initial thickness.

ℓ	$\hat{J}_{sp}(\mu^\ell)$	s_ℓ	$\|\hat{J}'_{sp}(\mu^\ell)\|_{L^2(\Omega)}$	$\langle \hat{J}'_{sp}(\mu^\ell), \mu_\delta \rangle_{L^2(\Omega)}$	
0	0.00377	—	0.4452	—	
1	0.00144	0.03125	0.1609	−0.445205	GM
2	0.00026	0.06250	0.0352	−0.033003	BFGS
3	0.00010	0.25000	0.0308	−0.001465	BFGS
4	0.00007	0.12500	0.0171	−0.001075	BFGS
5	0.00006	0.25000	0.0153	−0.000260	BFGS
6	0.00004	0.50000	0.0117	−0.000097	BFGS
7	0.00004	1.00000	0.0133	−0.000041	BFGS
8	0.00003	1.00000	0.0032	−0.000021	BFGS
9	0.00003	1.00000	0.0058	−0.000006	BFGS
10	0.00003	1.00000	0.0027	−0.000004	BFGS
11	0.00003	0.50000	0.0023	−0.000004	BFGS

TABLE 4.4. Run 4.2: Convergence results of the BFGS method for the non constant initial thickness.

Let us introduce the Banach space $Z = L^\infty(\Omega) \times V$ and the subset $Z_{ad} = \Lambda_{ad} \times V$, weher Λ_{ad} has been introduced in (2.6). We define the cost functional $\mathcal{J} : Z \to \mathbb{R}$

as

$$\mathcal{J}(z) = \int_\Omega \lambda(\mathbf{x}) + \frac{\eta}{2}\left|\lambda - \lambda^\circ\right|^2 + \beta\Phi\big(v(\mathbf{x}) - u_b(\mathbf{x})\big)\,\mathrm{d}\mathbf{x}$$

for $z = (\lambda, v) \in Z$. Furthermore, η, λ°, β, Φ, u_b are as in Sections 2.3 and 3.3.

We consider the optimization problem

$$\min \mathcal{J}(z) \quad \text{s.t.} \quad z \in \mathcal{F}(\mathbf{P}_{sur}), \tag{$\mathbf{P}_{sur}$}$$

where the feasible set is

$$\mathcal{F}(\mathbf{P}_{sur}) = \big\{z = (\lambda, v) \in Z_{ad} \,\big|\, c(\mu, v) = 0 \text{ and } \mu = \mathcal{P}(\lambda)\big\}.$$

We suppose that ($\mathbf{P}_{sur}$) has a local optimal solution $z^* = (\lambda^*, v^*) \in Z_{ad}$. In particular, we have $v^* = \mathcal{S}(\mathcal{P}(\lambda^*))$.

The corresponding reduced problem is given by

$$\min \hat{\mathcal{J}}(\lambda) \quad \text{s.t.} \quad \lambda \in \Lambda_{ad} \tag{$\hat{\mathbf{P}}_{sur}$}$$

with

$$\hat{\mathcal{J}}(\lambda) = \int_\Omega \lambda(\mathbf{x}) + \frac{\eta}{2}\left|\lambda - \lambda^\circ\right|^2 + \beta\Phi\big(\mathcal{S}(\mathcal{P}(\lambda))(\mathbf{x}) - u_b(\mathbf{x})\big)\,\mathrm{d}\mathbf{x}, \quad \lambda \in \Lambda_{ad}.$$

Next we derive formally first-order necessary optimality conditions for ($\mathbf{P}_{sur}$) without discussing constraint qualifications. Let the Lagrangian $\mathcal{L} : Z \times L^\infty(\Omega) \times V \times L^\infty(\Omega) \to \mathbb{R}$ be given by

$$\mathcal{L}(z, \mu, p, \xi) = \mathcal{J}(z) + \langle c(\mu, v), p\rangle_{V',V} + \int_\Omega \Big(\mu(\mathbf{x}) - \big(\mathcal{P}(\lambda)\big)(\mathbf{x})\Big)\xi(\mathbf{x})\,\mathrm{d}\mathbf{x}$$

for $z = (\lambda, v) \in Z$, $(\mu, p, \xi) \in L^\infty(\Omega) \times V \times L^\infty(\Omega)$. We suppose the following hypothesis.

Assumption 4. a) *There is a local solution $z^* = (\lambda^*, v^*) \in Z_{ad}$ to ($\mathbf{P}_{sur}$). Moreover, $\mu^* = \mathcal{P}(\lambda^*) \in M_{ad}$ satisfies $\mu_a(\mathbf{x}) < \mu^*(\mathbf{x}) < \mu_b(\mathbf{x})$ f.a.a. $\mathbf{x} \in \Omega$ (i.e., μ^* is an inactive solution).*

b) *The space mapping $\mathcal{P}$ is Fréchet-differentiable.*

c) *There exist Lagrange multipliers $p^* \in V$ and $\xi^* \in L^\infty(\Omega)$ satisfying*

$$\begin{aligned} \nabla_\lambda \mathcal{L}(z^*, \mu^*, p^*, \xi^*)(\lambda_\delta - \lambda^*) \geq 0 \qquad & \text{for all } \lambda_\delta \in \Lambda_{ad}, \\ \nabla_v \mathcal{L}(z^*, \mu^*, p^*, \xi^*)v_\delta = 0 \qquad & \text{for all } v_\delta \in V, \\ \nabla_\mu \mathcal{L}(z^*, \mu^*, p^*, \xi^*)\mu_\delta = 0 \qquad & \text{for all } \mu_\delta \in L^2(\Omega). \end{aligned}$$

From $\nabla_v \mathcal{L}(z^*, \mu^*, p^*, \xi^*)v_\delta = 0$ for all $v_\delta \in V$ we obtain the dual equation

$$\begin{aligned} -\mathrm{div}\left(2(1+n)\mu^*(\mathbf{x})\nabla p^*(\mathbf{x})\right) = -\beta\Phi'\big(v^*(\mathbf{x}) - u_b(\mathbf{x})\big) \qquad & \text{f.a.a. } \mathbf{x} \in \Omega, \\ p^*(\mathbf{x}) = 0 \qquad & \text{f.a.a. } \mathbf{x} \in \Gamma. \end{aligned}$$

Using $\nabla_\mu \mathcal{L}(z^*, \mu^*, p^*, \xi^*)\mu_\delta = 0$ for all $\mu_\delta \in L^\infty(\Omega)$ we find

$$\int_\Omega \big(2(1+n)\nabla v^*(\mathbf{x}) \cdot \nabla p^*(\mathbf{x}) + \xi^*(\mathbf{x})\big)\mu_\delta(\mathbf{x})\,\mathrm{d}\mathbf{x} = 0$$

which implies

$$\xi^*(\mathbf{x}) = -2(1+n)\nabla v^*(\mathbf{x}) \cdot \nabla p^*(\mathbf{x}) \quad \text{f.a.a. } \mathbf{x} \in \Omega.$$

Finally, $\nabla_\lambda \mathcal{L}(z^*, \mu^*, p^*, \xi^*)(\lambda_\delta - \lambda^*) \geq 0$ for all $\lambda_\delta \in \Lambda_{ad}$ yields

$$\begin{aligned}&\int_\Omega \Big(1 + \eta\big(\lambda^*(\mathbf{x}) - \lambda^\circ(\mathbf{x})\big)\Big)\big(\lambda_\delta(\mathbf{x}) - \lambda^*(\mathbf{x})\big) - \big(\mathcal{P}'(\lambda^*)(\lambda_\delta - \lambda^*)\big)(\mathbf{x})\xi^*(\mathbf{x})\,\mathrm{d}\mathbf{x}\\ &= \int_\Omega \Big(1 + \eta\big(\lambda^*(\mathbf{x}) - \lambda^\circ(\mathbf{x})\big) - \big(\mathcal{P}'(\lambda^*)^\star \xi^*\big)(\mathbf{x})\Big)\big(\lambda_\delta(\mathbf{x}) - \lambda^*(\mathbf{x})\big)\,\mathrm{d}\mathbf{x} \geq 0\end{aligned}$$

for all $\lambda_\delta \in \Lambda_{ad}$, where $\mathcal{P}'(\lambda^*)^\star$ is the adjoint operator to $\mathcal{P}'(\lambda^*)$.

It follows that the gradient $\hat{\jmath}'$ of the reduced cost functional is given by

$$\hat{\jmath}'(\lambda) = 1 + \eta(\lambda - \lambda^\circ) - \mathcal{P}'(\lambda)^\star \xi \quad \text{in } \Omega,$$

where ξ is given by

$$\xi = -2(1+n)\nabla v(\cdot)\cdot\nabla p(\cdot) \quad \text{in } \Omega, \tag{4.4}$$

the function v satisfies

$$\begin{aligned}-\mathrm{div}\,\big(2(1+n)\mu(\mathbf{x})\nabla v(\mathbf{x})\big) &= g(\mathbf{x}) \quad \text{f.a.a. } \mathbf{x} \in \Omega,\\ v(\mathbf{x}) &= 0 \qquad \text{f.a.a. } \mathbf{x} \in \Gamma\end{aligned} \tag{4.5}$$

with $\mu = \mathcal{P}(\lambda)$ and p is the solution to

$$\begin{aligned}-\mathrm{div}\,\big(2(1+n)\mu(\mathbf{x})\nabla p(\mathbf{x})\big) &= -\beta\Phi'\big(v(\mathbf{x}) - u_b(\mathbf{x})\big) \quad \text{f.a.a. } \mathbf{x} \in \Omega,\\ p(\mathbf{x}) &= 0 \qquad \text{f.a.a. } \mathbf{x} \in \Gamma.\end{aligned} \tag{4.6}$$

Inserting (4.4) we find

$$\hat{\jmath}'(\lambda) = 1 + \eta(\lambda - \lambda^\circ) + \mathcal{P}'(\lambda)^\star\big(2(1+n)\nabla v(\cdot)\cdot\nabla p(\cdot)\big) \quad \text{in } \Omega.$$

Let $\lambda \in \Lambda_{ad}$ and $\lambda_\delta \in L^\infty(\Omega)$ so that $\lambda + \lambda_\delta \in \Lambda_{ad}$. Then,

$$\mathcal{P}(\lambda + \lambda_\delta) \approx \mathcal{P}(\lambda) + \mathcal{P}'(\lambda)\lambda_\delta.$$

To avoid the computation of the operator $\mathcal{P}'(\lambda)$ we apply Broyden's updating formula providing a matrix B which can be used to replace $\mathcal{P}'(\lambda)$, but also $\mathcal{P}'(\lambda)^\star$.

We present the gradient projection method for $(\mathbf{P}_{sur})$ in Algorithm 3. For that purpose let $R : L^2(\Omega) \to \Lambda_{ad}$ be given by

$$R(\lambda) = \begin{cases}\lambda_a, & \text{where } \lambda \leq \lambda_a,\\ \lambda, & \text{where } \lambda_a \leq \lambda \leq \lambda_b,\\ \lambda_b, & \text{where } \lambda \geq \lambda_b\end{cases}$$

in the pointwise everywhere sense.

4.4. Numerical example for the surrogate optimization. We now discuss a numerical example using the surrogate optimization technique in combination with the space mapping technique from Section 4.1.

Run 4.3. For the surrogate optimization we follow the implementation strategy described in Algorithm 3. As a stopping criteria we use $\|\lambda(\tau_\ell) - \lambda(1)\|_{L^2(\Omega)} < \varepsilon_{abs}$, where ε_{abs} is given by the maximum triangle diameter of the discretization. The parameters η, β and λ° are set to 1.25, $25 \cdot 10^5$ and 1.2, respectively. This settings are very similar to the ones used in the linear optimaziation problem presented in Run 3.1. As bounds for the parameter λ we choose $\lambda_a = 0.05$ and $\lambda_b = 10$. Further we choose u_b to be 0.2. As initial thickness we use a constant thickness value $\lambda^0 = 0.75$. The settings for the space mapping are as described in Section 4.2. For the presented results we used the realization of space mapping using the truncated conjugate gradient method. In Figure 4.3 the results for the optimal thickness

Algorithm 3 (Gradient projection method for $(\mathbf{P}_{sur})$)

1: Choose initial $\lambda^0 \in \Lambda_{ad}$; set $\zeta = 10^{-4}$, $k = 0$, and $B_0 = \mathrm{id}_{L^2(\Omega)}$.
2: **repeat**
3: Compute $\mu^k = \mathcal{P}(\lambda^k)$.
4: Determine v^k from (4.5) with $\mu = \mu^k$ and evaluate $\hat{\jmath}(\lambda^k)$.
5: Compute p^k from (4.6) with $\mu = \mu^k$, $v = v^k$.
6: Evaluate the approximate gradient

$$D\hat{\jmath}^k = 1 + \eta(\lambda^k - \lambda^\circ) + B_k^\star\big(2(1+n)\nabla v^k(\cdot)\cdot\nabla p^k(\cdot)\big).$$

7: Determine a step length length parameter $\tau_k > 0$ so that

$$\hat{\jmath}\big(\lambda^k(\tau_k)\big) \le \hat{\jmath}(\lambda^k) - \frac{\zeta}{\tau_k}\,\|\lambda^k(\tau_k) - \lambda^k\|^2_{L^2(\Omega)}$$

where $\lambda^k(\tau) = R(\lambda^k - \tau D\hat{\jmath}^k) \in \Lambda_{ad}$.
8: Set $\lambda^{k+1} = \lambda^k(\tau_k)$ and use Broyden's formula to get

$$B_{k+1} = B_k + \frac{\mathcal{P}_\delta - B_k\lambda_\delta}{\|\lambda_\delta\|^2_{L^2(\Omega)}}\langle\lambda_\delta,\cdot\rangle_{L^2(\Omega)}$$

with $\lambda_\delta = \lambda^{k+1} - \lambda^k$ and $\mathcal{P}_\delta = \mathcal{P}(\lambda^{k+1}) - \mathcal{P}(\lambda^k)$.
9: Set $k = k + 1$.
10: **until** a certain stopping criterium is fulfilled

λ^* and the corresponding optimal displacement u^* of the p-Laplace equation are shown. Comparing the left plot of Figure 4.3 and Figure 4.4 we observe that

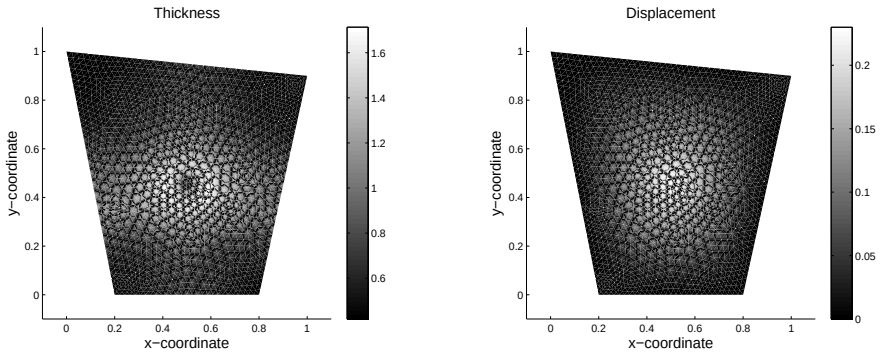

FIGURE 4.3. Run 4.3: Optimal thickness parameter λ_* (left plot) and the displacement $u_* = S(\lambda_*)$ computed from the non-linear (fine) model (right plot).

the maximal displacement of the non-linear is significantly larger than the maximal displacement for the linear model. Therefore, if we make the thickness parameter λ^* smaller, the maximal displacement for the non-linear model would be significantly larger than the threshold $u_b = 0.2$. The surrogate optimization takes this fact into account. From Figure 3.3 we can see that the optimal thickness parameter μ^* has a smaller scale compared to λ^*. The algorithm terminates after 11 iterations in

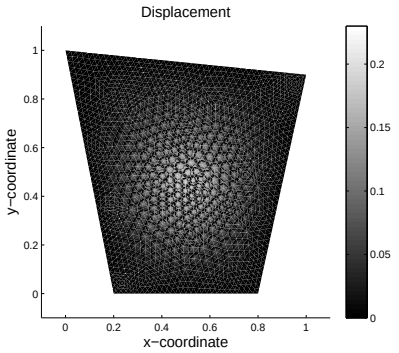

$\min_\Omega \lambda^*$	0.4187
$\max_\Omega \lambda^*$	1.7132
$\max_\Omega u^*$	0.2299
$\max_\Omega v^*$	0.1739
$\|u^* - v^*\|_{L^2(\Omega)}$	0.0195

FIGURE 4.4. Run 4.3: Displacement $v_* = \mathcal{S}(\lambda_*)$ obtain from the linear (coarse) model using the optmial thickness parameter μ^* (left plot) and optimization outputs (right table).

approximately 160 seconds. The convergence performance is presented in Table 4.5.

ℓ	$\hat{\mathcal{J}}(\lambda^\ell)$	τ_ℓ	$\|\lambda(\tau_\ell) - \lambda(1)\|_{L^2(\Omega)}$
0	12.02623556	—	—
1	5.88116959	0.0078125	62.12888484
2	1.34891305	0.5000000	9.67580780
3	1.32230609	0.5000000	1.58213312
4	0.92815629	0.0156250	56.83331364
5	0.78978949	0.2500000	0.79475753
6	0.78004224	0.0312500	2.23266634
7	0.76997875	0.0625000	0.28305133
8	0.76880665	0.1250000	0.09102810
9	0.76532536	0.0625000	0.13446468
10	0.76519108	0.0625000	0.04018094
11	0.76456476	0.0625000	0.02030304

TABLE 4.5. Run 4.3: Convergence results for the surrogate optimization.

APPENDIX

Proof of Lemma 3.4. To prove that the first Fréchet derivative of e is given by (3.3) we consider

$$\begin{aligned}
&\|c(y+y_\delta) - c(y) - c'(y)y_\delta\|_{V'} \\
&\quad = \sup_{\|\varphi\|_V=1} \int_\Omega 2(1+n)\mu_\delta(\mathbf{x})\nabla v_\delta(\mathbf{x}) \cdot \nabla\varphi(\mathbf{x})\,\mathrm{d}\mathbf{x} \le 2(1+n)\|\mu_\delta\|_{L^\infty(\Omega)}\|v_\delta\|_V \\
&\quad \le (1+n)\left(\|\mu_\delta\|^2_{L^\infty(\Omega)} + \|v_\delta\|^2_V\right) \le (1+n)\|y_\delta\|^2_Y,
\end{aligned}$$

where we have used the inequality $2ab \le a^2 + b^2$ for all $a, b \in \mathbb{R}$. Thus,

$$\lim_{\|y_\delta\|_X \to 0} \frac{1}{\|y_\delta\|_Y} \|c(y + y_\delta) - c(y) - c'(y)y_\delta\|_{V'} = 0$$

implies that (3.3) is the first Fréchet derivative.
Note that $y \mapsto c'(y)$ is a linear operator. Let $\mathcal{L}(Y, V')$ denote the Banach space of all linear and bounded operators from Y to V' endowed with the natural norm. From

$$\begin{aligned}\|c'(y)\|_{\mathcal{L}(Y,V')} &= \sup_{\|y_\delta\|_Y=1} \|c'(y)y_\delta\|_{V'} = \sup_{\|\varphi\|_V=1} \sup_{\|y_\delta\|_Y=1} \langle c'(y)y_\delta, \varphi\rangle_{V',V} \\ &\le 2(1+n) \sup_{\|y_\delta\|_Y=1} \Big(\|\mu_\delta\|_{L^\infty(\Omega)} \|v\|_V + \|\mu\|_{L^\infty(\Omega)} \|v_\delta\|_V \Big)\end{aligned}$$

and $\|y_\delta\|_Y = \|\mu_\delta\|_{L^\infty(\Omega)} + \|v_\delta\|_V = 1$ we infer that $c'(y)$ is a bounded operator for every $y \in Y$, i.e., $c'(y) \in \mathcal{L}(Y, V')$ for every $y \in Y$. Thus, $c'(y)$ is Fréchet-differentiable and its Fréchet derivative, which is the second Fréchet derivative of c, is given by (3.4). □

Proof of Proposition 3.5. Let $G \in V'$ be arbitrarily given. Then, $c_v(y)$ is a bijective operator if and only if there exists a unique $v_\delta \in V$ such that

$$c_v(y)v_\delta = G \quad \text{in } V'. \tag{A.1}$$

From (3.3) and (A.1) we obtain that the function v_δ satisfies

$$\int_\Omega 2(1+n)\mu(\mathbf{x})\nabla v_\delta(\mathbf{x}) \cdot \nabla\varphi(\mathbf{x})\,\mathrm{d}\mathbf{x} = \langle G, \varphi\rangle_{V',V} \quad \text{for all } \varphi \in V.$$

Now the claim follows from Proposition 3.1. □

Proof of Lemma 3.7. Since $v_b \in L^2(\Omega)$ holds and Φ is twice continuously differentiable, the mapping

$$v \mapsto \int_\Omega \Phi\big(v(\cdot) - v_b(\cdot)\big), \quad v \in V \subset L^2(\Omega)$$

is twice continuously Fréchet-differentiable and its first and second Fréchet derivative at v in any directions $v_\delta, \tilde{v}_\delta \in V$ read $\int_\Omega \Phi'(v(\cdot) - v_b(\cdot))v_\delta\,\mathrm{d}\mathbf{x}$ and $\int_\Omega \Phi''(v(\cdot) - v_b(\cdot))v_\delta\tilde{v}_\delta\,\mathrm{d}\mathbf{x}$, respectively. Since the first integral term of $\mathcal{J}$ is linear and bounded, the claim follows immediately. □

Proof of Theorem 3.8. From $\mu_a \le \mu_b$ we infer that $M_{ad} \neq \emptyset$. Using $\mu_a > 0$ and Proposition 3.1 we infer that $\mathcal{F}(\mathbf{P}_c) \neq \emptyset$. Moreover,

$$0 < \int_\Omega \mu_a\,\mathrm{d}\mathbf{x} \le \inf_{y \in \mathcal{F}(\mathbf{P}_c)} \mathcal{J}(y) < \infty.$$

Suppose that $\{y^k\}_{k\in\mathbb{N}}$ with $y^k = (\mu^k, v^k)$ is a minimizing sequence in $\mathcal{F}(\mathbf{P}_c)$. Then, $\{\mu^k\}_{k\in\mathbb{N}}$ lies in M_{ad}. Therefore, this sequence is bounded in $L^\infty(\Omega)$, in particular, in $L^2(\Omega)$. From (3.2) and Assumption 1, part 2), we conclude that there exists an element $y^* = (\mu^*, v^*) \in Y$ and a subsequence $\{y^{k_j}\}_{j\in\mathbb{N}}$, $y^{k_j} = (\mu^{k_j}, v^{k_j})$, so that

$$\mu^{k_j} \rightharpoonup \mu^* \text{ in } L^2(\Omega) \text{ for } j \to \infty, \tag{A.2a}$$

$$v^{k_j} \rightharpoonup v^* \text{ in } H^s(\Omega) \cap V \text{ for } j \to \infty. \tag{A.2b}$$

Since M_{ad} is closed and convex in $L^2(\Omega)$, we have $\mu^* \in M_{ad}$. Utilizing Remark 3.2, part 2), we infer that u^{k_j} converges stronly to v^* in V for $k \to \infty$. Thus,

$$\lim_{j\to\infty} \langle c(y^{k_j}) - c(y^*), \varphi\rangle_{V',V} = 0 \quad \text{for all } \varphi \in V.$$

Due to $c(y^{k_j}) = 0$ in V' we find $c(y^*) = 0$ in V', so that $y^* \in \mathcal{F}(\mathbf{P}_c)$ holds. Recall that norms are weakly lower semi-continuous (see, e.g., [19, p. 377]) as well as that $\mu^{k_j}(\mathbf{x}) \geq \mu_a > 0$ f.a.a. $\mathbf{x} \in \Omega$ and j. By (A.2a), the sequence $\{\mu^{k_j}\}_{j\in\mathbb{N}}$ converges weakly in $L^1(\Omega)$. Using $\mu^* \in M_{ad}$ we have

$$\lim_{j\to\infty} \int_\Omega \mu^{k_j}\,\mathrm{d}\mathbf{x} = \lim_{j\to\infty} \|\mu^{k_j}\|_{L^1(\Omega)} \geq \|\mu^*\|_{L^1(\Omega)} = \int_\Omega \mu^*(\mathbf{x})\,\mathrm{d}\mathbf{x}$$

Recall that norms are weakly lower semi-continuous; see, e.g., [19]. Utilizing Assumption 1-a) and (A.2b) we conclude

$$\inf_{y\in\mathcal{F}(\mathbf{P}_c)} \mathcal{J}(y) = \lim_{j\to\infty} \mathcal{J}(y^{k_j}) \geq \mathcal{J}(y^*)$$

which gives the claim. □

Proof of Theorem 3.10. Due to Remark 3.6 there exists a Lagrange multiplier $p^* \in V$ satisfying together with the optimal solution $y^* \in Y_{ad}$

$$\nabla_\mu L(y^*, p^*)(\mu_\delta - \mu^*) \geq 0 \qquad \text{for all } \mu_\delta \in M_{ad}, \tag{A.3a}$$

$$\nabla_v L(y^*, p^*)v_\delta = 0 \qquad \text{for all } v_\delta \in V, \tag{A.3b}$$

$$\nabla_p L(y^*, p^*)p_\delta = \langle c(y^*), p_\delta\rangle_{V',V} = 0 \qquad \text{for all } p_\delta \in V; \tag{A.3c}$$

see, e.g., [16, 17]. From (3.6) and (A.3a) we obtain (3.8). Utilizing (3.6) and (A.3b) it follows that

$$\int_\Omega \big(2(1+n)\mu^*(\mathbf{x})\nabla v_\delta(\mathbf{x})\big)\cdot\nabla p^*(\mathbf{x})\,\mathrm{d}\mathbf{x} = -\int_\Omega \beta\Phi'\big(v^*(\mathbf{x}) - v_b(\mathbf{x})\big)\,v_\delta(\mathbf{x})\,\mathrm{d}\mathbf{x} \tag{A.4}$$

for all $v_\delta \in V$. Thus, $p^* \in V$ is the weak solution to the linear, elliptic problem (3.7). It follows from Proposition 3.1 that p^* is uniquely determined. □

References

[1] R.A. Adams. *Sobolev Spaces*. Academic Press, New York-London, 1975. Pure and Applied Mathematics, Vol. 65.

[2] W. Ames. *Nonlinear Partial Differential Equations in Engineering*. Academic Press, New York, 1965.

[3] R. Aris. *The Mathematical Theory of Diffusion and Reaction in Permeable Catalysts*. Vols. 1 and 2, Clarendon Press, Oxford, 1975.

[4] M.H. Bakr, J.W. Bandler, K. Masden, and J. Søndergaard. An introduction to the space mapping technique. *Optimization and Engineering*, 2, 369-384, 2001.

[5] J.W. Bandler, R.M. Biernacki, S.H. Chen, P.A. Grobelny, and R.H. Hemmers. Space mapping technique for electromagnetic optimization. *IEEE Trans. Microwave Theory Tech.*, 42: 2536-2544, 1994.

[6] J.W. Bandler, R.M. Biernacki, S.H. Chen, R.H. Hemmers, and K. Madsen. Electromagnetic optimization exploiting agressive space mapping. *IEEE Trans. Microwave Theory Tech.*, 43:2874-2882, 1995.

[7] E. Casas and L.A. Fernández. Dealing with integral state constraints in boundary control problems or quasilinear elliptic equations. *SIAM J. Control and Optimization*, 33:568-589, 1995.

[8] E. Casas and L.A. Fernández. Distributed control of systems governed by a general class of quasilinear elliptic equations. *J. Differential Equations*, 104:20-47, 1993.

[9] J.I. Diaz. *Nonlinear partial differential equations and free boundaries*. Vol. I, Elliptic equations, Research Notes in Math., Vol. 106, Pitman, London, 1985.
[10] I. Ekeland and R. Temam. *Convex Analysis and Variational Problems*. North-Holland Publishing Company, Amsterdam, 1972.
[11] L.C. Evans. *Partial Differential Equations*. Graduate Studies in Mathematics, vol. 19, American Mathematical Society, Providence, Rhode Island, 2002.
[12] M. Hintermüller and L.N. Vicente. Space mapping for optimal control of partial differential equations. *SIAM J. Optimization*, 15:1002-1025, 2005.
[13] C.T. Kelley. *Iterative Methods for Optimization*. Frontiers in Applied Mathematics. SIAM, Philadelphia, 1999.
[14] O. Lass. Efficient numerical space mapping techniques for the p-Laplace equation. Diploma thesis, Institut für Mathematik und Wissenschaftliches Rechnen, Karl-Franzens Universität Graz, in preparation, 2009.
[15] S.J. Leary, A. Bhaskar, and A.J. Keane. A constraint mapping approach to the structural optimization of an expensive model using surrogates. *Optimization and Engineering*, 2, 385-398, 2001.
[16] D.G. Luenberger. *Optimization by Vector Space Methods*. John Wiley & Sons, Inc.,New York, 1969.
[17] H. Maurer and J. Zowe. First and second order necessary and sufficient optimality conditions for infinite-dimensional programming problems. *Mathematical Programming* **16** (1979), 98-110.
[18] J. Nocedal and S. J. Wright. *Numerical Optimization*. 2. Auflage, Springer Series in Operation Research. Springer-Verlag, New York, 2006.
[19] M. Reed and B. Simon *Methods of Modern Mathematical Physics. Volume 1: Functional Analysis*. Academic Press, Inc., Boston, 1980.
[20] G. Scharrer, S. Volkwein, and T. Heubrandtner. Mathematical optimization of a plate volume under a p- Laplace partial differential equation constraint by using standard software. Submitted, 2009.
[21] G.M. Troianiello. *Elliptic Differential Equations and Obstacle Problems*. Plenum Press, New York, 1987.
[22] L.N. Vicente. Space mapping: models, sensitivities, and trust-region methods. *Optimization and Engineering*, 4:159-175, 2003.

O. Lass, Universität Graz, Institut für Mathematik und Wissenschaftliches Rechnen, Heinrichstrasse 36, A-8010 Graz, Austria
E-mail address: oliver.lass@edu.uni-graz.at

C. Posch, Universität Graz, Institut für Mathematik und Wissenschaftliches Rechnen, Heinrichstrasse 36, A-8010 Graz, Austria
E-mail address: cornelia.posch@edu.uni-graz.at

G. Scharrer, The Virtual Vehicle Competence Center, Inffeldgasse 21a, A-8010 Graz, Austria
E-mail address: georg.scharrer@virtuellesfahrzeug.at

S. Volkwein, Universität Konstanz, Fachbereich Mathematik und Statistik, Universitätsstrasse 10, D-78457 Konstanz, Germany
E-mail address: Stefan.Volkwein@uni-konstanz.de